UNIVERSIDAD DE INVESTIGACIÓN DE TECNOLOGÍA EXPERIMENTAL YACHAY

Escuela de Ciencias Físicas y Nanotecnología

Complex Behaviors in Artificial Societies

Trabajo de integración curricular presentado como requisito para la obtención del título de Físico/a.

Autor:

Brandon André Minta Gómez

Tutor:

Mario Cosenza, PhD.

Urcuquí, abril 2024

Autoría

Yo, **Brandon André Minta Gómez**, con cédula de identidad 1725096802 declaro que las ideas, juicios, valoraciones, interpretaciones, consultas bibliográficas, definiciones y conceptualizaciones expuestas en el presente trabajo; así cómo, los procedimientos y herramientas utilizadas en la investigación, son de absoluta responsabilidad de el/la autora (a) del trabajo de integración curricular. Así mismo, me acojo a los reglamentos internos de la Universidad de Investigación de Tecnología Experimental Yachay.

Urcuquí, Abril 2024.

Brandon André Minta Gómez
CI: 1725096802

AUTORIZACIÓN DE PUBLICACIÓN

Yo, **Brandon André Minta Gómez**, con cédula de identidad 1725096802 cedo a la Universidad de Investigación de Tecnología Experimental Yachay, los derechos de publicación de la presente obra, sin que deba haber un reconocimiento económico por este concepto. Declaro además que el texto del presente trabajo de titulación no podrá ser cedido a ninguna empresa editorial para su publicación u otros fines, sin contar previamente con la autorización escrita de la Universidad.

Asimismo, autorizo a la Universidad que realice la digitalización y publicación de este trabajo de integración curricular en el repositorio virtual, de conformidad a lo dispuesto en el Art. 144 de la Ley Orgánica de Educación Superior.

Urcuquí, Abril 2024.

_____
Brandon André Minta Gómez
CI: 1725096802

Dedication

To my lovely mother.

Acknowledgements

This thesis stands as a testament not only to my academic journey, but also to the unwavering support and love of my family. To my mother, Jessenia, a beacon of strength, wisdom and love. Despite the difficulties we faced, you always gave the best to us, your children. Your unwavering support and protection have been my sanctuary, your love my sustenance. To my father, Efrain, your reasonable advice and desire for my success have been the compass guiding my decisions. To my brothers, Benjamin and Brian, who have been my constant companions through life's highs and lows. Your faith in me has often been the wind beneath my wings.

To my mentor and tutor, Professor Mario Cosenza, who opened my eyes to the fascinating world of Complex Systems and Physics, I owe a debt of gratitude. Your passion and dedication have inspired me to delve deeper and reach further.

I extend my heartfelt thanks to all the professors who have imparted their knowledge and sparked my curiosity. The pleasure of being a physicist is a gift that you have bestowed upon me.

To my friends, who made this journey not just bearable, but enjoyable, I am forever grateful. A special mention to Osmer and Jonnathan, whose camaraderie and support have been invaluable.

Lastly, I acknowledge CEDIA for providing access to the HPC facilities, which were instrumental in the simulations for this thesis.

To all who have contributed to my life, I offer my deepest gratitude. Your impact extends far beyond the pages of this thesis. Thank you all.

<div align="right">Brandon Minta Gómez</div>

Resumen

Implementamos una simulación computacional a escala completa del Modelo de Tributo y Conflicto de Axelrod dentro de la perspectiva contemporánea e interdisciplinar de los sistemas complejos y exploramos los comportamientos colectivos emergentes a través del análisis estadístico de sus resultados. Investigamos el Modelo de Tributo de Axelrod en una situación realista de una red bidimensional. Se abordan varias cuestiones de interés: la distribución de frecuencias y tamaños de los conflictos, la distribución de frecuencias entre eventos de grandes conflictos, la evolución y distribución de recursos, el surgimiento y caída de coaliciones, entre otras. Generalizamos el modelo original en dos aspectos: (i) al considerar una red global de interacciones, y (ii) al introducir un decaimiento exponencial en el rango de interacciones. Analizamos los efectos de los distintos parámetros del modelo sobre la aparición de comportamientos colectivos en el sistema calculando diversos diagramas de fases. Investigamos la formación de coaliciones o alianzas utilizando conceptos de redes complejas sobre la red de compromisos adaptativa resultante. Visualizamos las redes de compromisos entre agentes, revelando la formación de coaliciones como estructuras modulares. Se introduce el índice de Gini para caracterizar la distribución de recursos en el sistema a lo largo de su evolución. Descubrimos una correlación entre la disponibilidad de recursos y los conflictos sociales. Identificamos parámetros del modelo que pueden contribuir a reducir la desigualdad resultante de los conflictos. Nuestra exploración extiende las ideas originales de Axelrod a un contexto más amplio, ampliando nuestra comprensión de las complejas dinámicas sociopolíticas y sus implicaciones para la sostenibilidad global.

Palabras clave: Sistemas complejos; Sociofísica, Dinámica de conflictos; Auto-organización, Sostenibilidad.

Abstract

We implement a full scale computational simulation of Axelrod's Tribute and Conflict Model within the contemporary and interdisciplinary perspective of complex systems and explore the emerging collective behaviors through statistical analysis of its outcomes. We investigate Axelrod's Tribute Model in a realistic situation of a two dimensional lattice. Several issues of interest are addressed: the frequency distribution and sizes of the conflicts, the frequency distribution of inter-event of large conflicts, the evolution and distribution of resources, the rise and fall of coalitions, among others. We generalize the original model in two aspects: (i) by considering a global network of interactions, and (ii) by introducing an exponential decay on the range of interactions. We analyze the effects of the various parameters of the model on the emergence of collective behaviors in the system by calculating diverse phase diagrams. We investigate the formation of coalitions or alliances by using concepts from complex networks on the resulting adaptive network of commitments. We visualize the networks of compromises between agents, revealing the formation of coalitions as modular structures. The Gini index is introduced to characterize the distribution of resources in the system along its evolution. We uncover a correlation between resource availability and social conflicts. We identify parameters of the model that can contribute to reduce inequality resulting from conflicts. Our exploration extends Axelrod's original insights to a broader context, expanding our understanding of complex sociopolitical dynamics and their implications for global sustainability.

Keywords: Complex Systems; Sociophysics, Conflict dynamics; Self-organization, Sustainability.

Contents

List of Figures

List of Tables

Chapter 1

Introduction

The term 'complex' originates in the Latin roots 'com', signifying 'together', and 'plectere', which means 'to weave' [1]. This etymology encapsulates the essence of complex systems, characterized by many interconnected elements working in unison. However, the study of these systems transcends mere observation of individual components. It delves into the intricate relationships and interactions that give rise to emergent properties.

In recent years, Physics and other sciences have created the general concept of complex system to describe a diversity of natural and artificial systems. A *complex system* [2][3] is a set of interacting elements whose collective behavior cannot be derived from the knowledge of the properties of the isolated elements. The collective behavior is said to emerge from the interactions between the components, without any external influence or design. These systems commonly exhibit two properties: self-organization and emergence. The first one corresponds to the display of organization without the application of an external organizing principle or rule. The second is the manifestation of properties that are not present in the constituents of the system nor can be described by the superposition of their properties. A paradigmatic example of a complex system is the brain. It is well known how a single neuron functions. A single neuron cannot think nor have consciousness by itself, but a network of billions of them forming the brain can give rise to thought, conscience, and emotions. The concept of complex system takes on another interesting form in social systems, where human interactions can lead to the emergence of social and political structures. The application of the concepts and methods of complex systems to study social systems has been called *Sociophysics* [4].

Doran and Gilbert [5] assert that "computer simulation is an appropriate methodology whenever a social phenomenon is not directly accessible". This approach is especially pertinent when confronting complex systems where direct observations may prove impractical. Using computer simulations, researchers can effectively model intricate dynamics and interactions that would otherwise be challenging to study. For instance, social interaction processes are so complex that it is practically impossible to model all aspects of the target phenomena. This complexity arises from a society comprising numerous heterogeneous and restricted minds, each contributing to the intricate tapestry of social dynamics.

A model conceptualized and shaped as a computer simulation has been termed an 'Artificial Society.' Such entities are neither better nor worse than the real world; they exist as distinct entities within the world, possessing a notable degree of autonomy. The refined observation they provide sets artificial societies apart from the real world. Unlike the complexities inherent in real-world phenomena, artificial societies offer a simpler way for examining and exploring different structures and behaviors. This facilitates improving our knowledge and understanding of potential social worlds along with exploratory simulations.

Conte and Gilbert[5] perspectives on social actions extend beyond the dichotomy of cooperation and conflict. Certain social actions exhibit clear advantages or disadvantages, and a complex hierarchy of goals governs them. In this context, the study of Artificial Societies becomes invaluable for examining the nature of social interactions. Social interference describes structural social relations as "self-sufficient agents in a common world hindering or facilitating one another"[5].

The emergence of organization, alliances, and coalitions in societies is a problem of great interest that has been approached in the context of complex systems. This is a vital issue in today's world, since we are experiencing an era in which the standard political unit, the nation, is no longer completely stable. We see, on the one hand, how some states have disintegrated, like the Soviet Union and Yugoslavia; while on the other hand, large entities have appeared, such as the European Union, NATO, the UN, the OAS, Mercosur, and other regional associations, to achieve greater stability and socioeconomic sustainability. The problem of the grouping and segregation of structures and alliances is essential for understanding the global geopolitics.

Many models have assumed from the outset the presence of community organizations and, therefore, do not propose mechanisms to explain how these organized structures could appear. Traditionally, the fundamental paradigm of models for the formation of social structures or coalitions has been game theory[6]. This theory assumes knowledge of who the agents are in a system, and the strategies they adopt in very particular conditions; but the agents do not spontaneously form alliances or organized structures.

In the post-Cold War era, the prominent social scientist Robert Axelrod proposed a model in an influential article titled *Building New Political Actors*[7] that describes the process by which independent agents might relinquish part of their autonomy, creating a new entity at a higher level of organization.

Axelrod's Tribute and Conflict Model[7] uses techniques and concepts from complex adaptive systems[23]. Axelrod's work can be considered as an alternative approach within the field of political and social sciences in the study of the emergence of states and alliances organized through processes based on local interactions with well-defined rules between units or elementary agents. As a result from these interaction processes, collective properties emerge in the system, such as as higher levels of organization, formation of structures and patterns. The purpose of Axelrod's model is to explain the process of formation of coalitions or alliances based on simple rules of lo-

cal interaction. The emergency of self-organized collective states (what Axelrod calls new political actors), not only occurs within a social or political context, but also appears in a wide variety of phenomena in nature, such as in biological systems, where organs and tissues arise from single-celled organisms; or the way the brain's neurons are connected to produce sophisticated mental functions, such as memory, logical reasoning or consciousness[2][3].

The dynamics of aggregation and fragmentation of influential agents become pivotal for comprehending the future of global politics, encompassing international security affairs and political economy. Axelrod's Tribute Model[7] mirrors the historical state-formation processes through a "pay or else" strategy through which states formation can be analyzed via extortion and compromise, shedding light on how nations can become less egotistical for collective action. This model serves as a theoretical framework to describe diverse troubled situations that involve power relations; from the rise of empires, mafia organizations, conflicts among nations, the dynamics of warfare, to personal relations and negotiations. Axelrod's model allows to investigate the emergence of higher organizational levels, to delineate their minimal conditions for existence, to comprehend survival behaviors and collapses, and helps to unveil phenomena of significance for the broader study of international politics, Sociophysics, and Econophysics.

1.1   Problem Statement

Motivated by the relevance of the problem of the prevalence of conflicts and formation of alliances in today's world, in this Thesis we undertake the task of implementing a full scale computational simulation of Axelrod's Tribute Model within the perspective of complex systems and explore its consequences through statistical analysis of its outcomes. We investigate Axelrod's Tribute Model in a realistic situation of two dimensions and in other connectivity topologies, applying the rules of interaction through extended numerical simulations. We address several issues of interest: the frequency distribution and sizes of the conflicts, the frequency distribution of peace intervals, the evolution and distribution of resources, the rise and fall of coalitions, among others. Our exploration aims to extend Axelrod's original insights into a broader context, expanding our understanding of complex sociopolitical dynamics and their implications for global sustainability. The present Thesis is framed within the contemporary interdisciplinary field of complex systems.

1.2   Objectives

1.2.1   General Objective

To implement Axelrod's Tribute Model on a full scale through computational simulations and to investigate its consequences by using concepts and techniques from Statistical Physics and Complex Systems.

1.2.2   Specific Objectives

- Apply the fundamental concepts of Axelrod's Tribute Model on a two-dimensional lattice.

- Generalize Axelrod's Tribute Model to a globally coupled network and by varying the range of interaction.

- Analyze statistically the collective behaviors emerging along the evolution of the systems.

- Identify the parameters and strategies that influence the formation of alliances or aggregates of agents, the distribution of conflicts and peace intervals, and the distribution of resources.

- Introduce novel visualization techniques of the resulting compromises between agents by using complex network tools.

1.3   Overview

Chapter 2 contains the theoretical framework on which the present Thesis is based. We present a review of the concepts employed in this Thesis, encompassing complex networks, adaptive networks, agent-based models, models of social interaction, and the landscape theory of aggregation. We provide a formal definition of Axelrod's Tribute Model that we shall develop in this Thesis. Chapter 3 presents the implementation of the Tribute model on a two-dimensional square lattice. The collective behaviors arising in the system are analyzed in this Chapter, uncovering universal features such as heavy tail distributions that govern the inter-time distribution of conflicts. This Chapter also includes the visualization of the commitment patterns among the agents. Chapter 4 extends the application of the tribute model to a global network, analyzing the nature of conflicts, conflict sizes, and visualizing the dynamical patterns. In Chapter 5 we propose an extension of the rules of the original Axelrod model. We simplify the target selection process by fitting the range of interaction from empirical data. We obtain an exponentially decaying range of interaction that we apply in order to construct various phase diagrams. Finally, Chapter 6 presents the conclusions of our work, spotlighting significant findings and providing insights for future research. The appendix includes the Python codes elaborated by the author of this Thesis for simulations and visualizations, facilitating the replication of our study.

Chapter 2

Theoretical framework

2.1 Complex Networks

Social networks can be represented as intricate structures where nodes represent individuals or groups, and the edges denote social interactions, encompassing aspects such as empathy, collaboration, or conflict[8]. In our interconnected world, studying these networks is vital for understanding social interactions and structures, especially within platforms like X, Facebook, Instagram, WhatsApp[9].

The roots of social network analysis trace back to psychiatrist Jacob Moreno in the 1930s, who introduced the earliest studies in what later evolved into "sociometry" and, eventually, complex system analysis. Figure 2.1(a) showcases Moreno's hand-drawn *sociogram* of a 4th-grade class, representing the precursor to modern social network visualizations. Over time, the field has flourished, marked by numerous constructed and studied social networks. Wayne Zachary's renowned study[10] offers a case in point, portraying the friendship connections among 34 members of a North American karate club (see Figure 2.1(b).
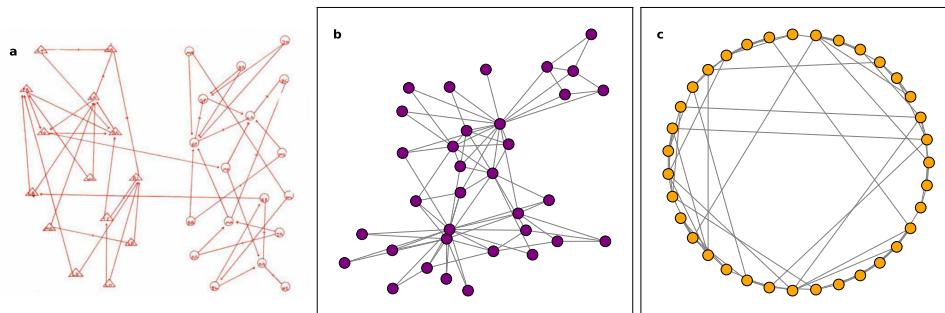

Figure 2.1: **Social Networks:** a) Sociogram illustrating the class structure of a 4th-grade with 17 boys (triangles) and 16 girls (circles)[11]. b) Graph depicting the friendship connections among 34 members of Zachary's Karate Club[10]. c) Small world network with $N = 35, k = 4, p = 0.3$.

In essence, a network is a set of nodes connected by edges[3]. The representation of networks often involves an adjacency matrix, where rows and columns correspond to nodes. In this context, the presence of an edge between nodes i and j is denoted by a_{ij}, designating node j as a neighbor of node i. Networks exhibit various classifications based on the nature of their edges:

- **Undirected Graph** Symmetric connections characterize undirected edges, where nodes i and j are mutually connected.

- **Directed Graph** Asymmetric connections define directed edges, connecting node i to node j without necessitating a reciprocal link.

- **Unweighted graph** Here, the edges only represent if there is or is not a connection between nodes.

- **Weighted graph** In this graph, each edge possesses a weight, quantifying the intensity of the connection between nodes.

- **Multiple Edges** Edges with the same origin and destination

Another important aspect of complex networks is the concept of **community** and **modularity**. A *community* is defined as a subset of nodes more densely connected within the network than others, and these communities may overlap with one another. An exemplary illustration of community detection is presented in Figure 2.2, showcasing the division of Zachary's Karate Club into distinct communities. This concept finds practical application in network businesses, for example, where elements operate within similar economic sectors.

In contrast, modularity refers to organizing the network into multiple communities. The modularity (Q) is mathematically defined as:

$$Q = \frac{|E_{in}| - <|E_{in}|>}{|E|}$$

Here, $|E|$ represents the total number of edges, $|E_{in}|$ is the number of edges within communities that do not cross boundaries, and $<|E_{in}|>$ is the expected number of edges within the community in random topology.

A renowned algorithm for identifying communities is the *Louvain method*[12], designed to maximize modularity. This approach has proven effective in discerning intricate community structures within complex networks.

Beyond the intrinsic nature of individual components and their connections, understanding the patterns of interaction is pivotal for grasping system behavior. In social networks, these interaction patterns wield significant influence, shaping phenomena such as spreading diseases or disseminating opinions within populations.

Acknowledging a network's role as a simplified representation with essential pattern connections underscores its abstraction, a strategic simplification that brings notable advantages despite omitting intricate details. Hubs, characterized by nodes boasting a high degree, assume a pivotal role in shaping network performance, especially within social contexts where a select few individuals command extensive connections. A nuanced exploration and comprehension of these hubs prove fundamental for understanding the network's intricate dynamics.

Concluding this exploration of network phenomena, the "small world effect," vividly captured in Figure 2.1(c), commonly referred to as the "six degrees of separation," asserts that a network with no more than five intermediaries facilitates global communication, establishing links between any two individuals.
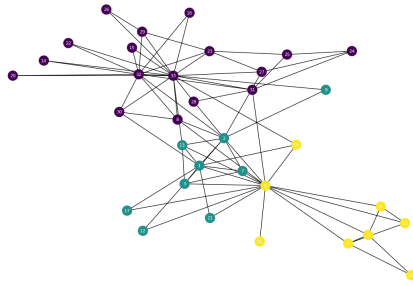
Figure 2.2: **Zachary's Karate Club Network:** Community Detection

Continuing on networks, adaptive networks emerge as a significant class among different dynamical network models. These models, described as those illustrating the co-evolutionary dynamics of systems, capture the subtle interplay where node states and typologies mutually adapt and change in response to each other's dynamics over time[3].

An illustrative example of an adaptive network is portrayed in Figure 2.3, featuring a Susceptible-Infected-Susceptible (SIS) model—a representative epidemiological model consisting of two groups, susceptible and infected. In this model, susceptible nodes can contract infection from their infected neighbors with a probability p_i. Moreover, a chance exists for a susceptible node to sever its existing edge and rewire with a new node, a decision governed by the severance probability p_s. Infected nodes may also recover to a susceptible state, determined by the probability p_r.
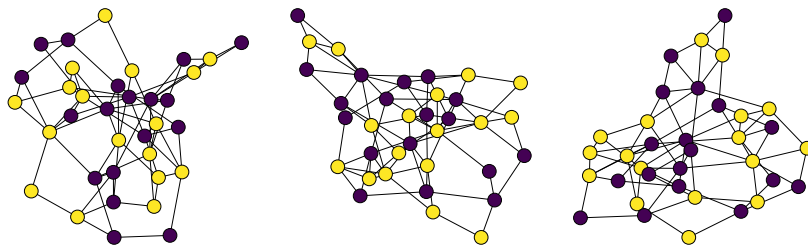
Figure 2.3: **SIS Adaptive Network Evolution:** The simulation features 35 nodes, with infection probability (p_i) set at 0.5, recovery probability (p_r) at 0.2, and severance probability (p_s) at 0.5. The temporal progression is depicted from left to right

Extending the scope to the evolution of social communities, nodes within adaptive networks represent individuals with specific social-cultural states or properties. Edges, denoting social interactions, dynamically shift through the entry or withdrawal of individuals within the community. This subtle interplay captures the evolving fabric of social networks, where adaptive mechanisms shape the ever-changing landscape of connections and interactions.

2.2   Agent Based Models

Agent-based models (ABMs) are versatile tools for modeling complex systems across various disciplines, including economics, social science, ecology, and biology. While the specific constraints defining the structure of an ABM are not rigidly defined, Sayama outlines fundamental general properties[3]:

- **Discrete:** The model operates in a discrete space, representing individual entities as distinct agents.

- **Internal States:** Agents possess internal states that dictate their behavior and interactions.

- **Spatially Localized:** Agents are situated within a spatial context, allowing for localized interactions.

- **Interaction and Perception:** Agents interact with and perceive their surroundings, influencing their decision-making.

- **Guided Actions:** Agents exhibit actions by predetermined behavioral guidelines.

- **Interaction with Others:** Agents interact with other agents, contributing to the emergent system dynamics.

- **Collective Behavior:** The model may produce nontrivial "collective behavior" arising from the interactions of individual agents.

The distinctive feature of ABMs lies in describing agent behavioral rules algorithmically rather than through explicit mathematical formulations. While this approach provides a good representation of complex systems, it does pose challenges to analytical tractability. Due to the inherent complexity of ABMs, conducting elegant mathematical analyses becomes challenging. Consequently, analyzing ABMs and their simulation results involves testing to identify significant differences under various experimental conditions.

As highlighted by Axelrod[13], the primary goal of ABMs is not predictive accuracy but rather a means to comprehend complex social processes. ABMs offer a framework for exploring and understanding emergent phenomena within social systems, acknowledging the inherent complexity that defies straightforward mathematical analysis.

2.3   Social-Interaction models

Schelling's segregation model[14] is a pioneering and paradigmatic ABM model and constitutes a valuable tool for examining social segregation. This model adopts an Ising-like structure, initially implementing a lattice of size N with a Moore neighborhood. The automaton, a term denoting a theoretical machine that evolves its internal states based on preceding states[3], operates with states $S = \{A, B, O\}$. Here, A and B signify two distinct types of agents within a cell, while O designates empty spaces.

Initially, the unoccupied cells represent a fraction $\rho = N_0/N^2$ and agents of different types randomly occupy the remaining sites. At each step, an agent evaluates its surroundings, computing the fraction of agents of its type. If this fraction falls below a predefined threshold, the agent relocates to an empty site. Figure 2.4 illustrates the emergence of clusters comprised of agents of the same type.
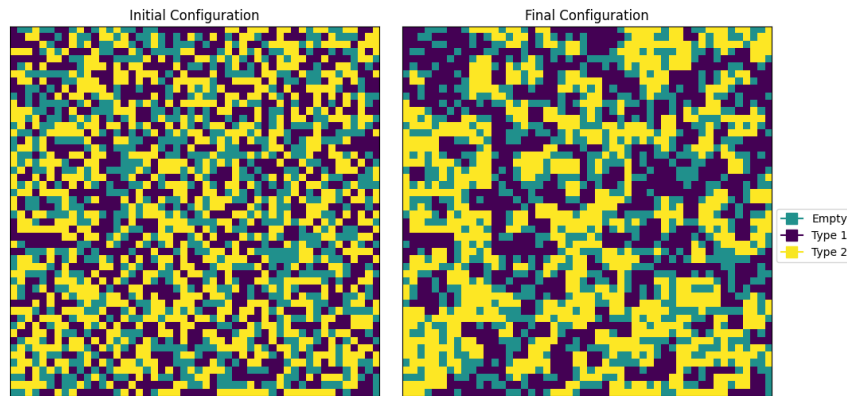
Figure 2.4: **Schelling's Segregation Model:** Replication in a 50x50 lattice: Initial and Final Configurations. $\rho = 0.3$

Examining different scenarios of social dynamics, we can further explore the subtleties of strategic decision-making through the lens of classic game theory, as exemplified by the renowned Prisoner's Dilemma. Introduced by the American mathematician Merrill Flood, the Prisoner's Dilemma is a clear example of cooperation dynamics among rational players. Numerous studies, including the notable work by Axelrod[15], have delved into strategies for effective gameplay within this paradigm. The scenario of the Prisoner's Dilemma unfolds with two individuals committing a crime together, subsequently placed in separate cells with no means of communication. As a prosecutorial tactic, authorities reward either prisoner for providing evidence against the other. The three possible outcomes are as follows:

- One criminal defects and the other cooperates (remains silent), leading to the former's release and the latter's sentencing to 3 years in prison.

- If both prisoners defect, each receives a 2-year prison sentence.

- If both prisoners cooperate, insufficient evidence exists for conviction, resulting in a shared 1-year prison term.

2.4   The Landscape Theory of Aggregation

Axelrod's assertion that "politics minimizes the strangeness of bedfellows"[13] suggests that alliances can form between seemingly disparate entities when politically advantageous. The Landscape theory of aggregation further explores this concept, examining how elements within a system align themselves based on compatibility and distance, adding a layer of complexity to system configurations and interactions. This theory has far-reaching implications, influencing international power dynamics and setting quality benchmarks in competitive industries. It offers insights into potential international alignments and underscores the volatility of domestic political coalitions, leading to system changes.

The Landscape theory initiates with *n* nations or agents, each characterized by a size $s_i > 0$, reflecting demographics, economics, armament status, or a significant combination thereof. Propensity p_{ij} denotes the inclination of two nations, *i* and *j*, to collaborate, with larger values indicating a higher likelihood of collaboration and lower/negative values representing potential conflicts. To ensure symmetry in considering conflicts, $p_{ij} = p_{ji}$. The theory has two main assumptions: a"myopic" nature of national leadership in performance evaluations and the gradual realignment of nations due to ambiguous benefits. These assumptions present negotiation challenges as potential outcomes remain uncertain, providing a deeper understanding of international relations and power balance dynamics.

Configuration is defined as *X*, representing the grouping of nations and the associated distance d_{ij} between pairs. In hierarchical organizations, the distance signifies the number of layers. A binary representation is commonly used, with 0 denoting group membership and 1 indicating disjointedness.

As proposed by Axelrod[13], the notion of "frustration" emerges, capturing how well or poorly a configuration satisfies a nation or agent. Nations seek configurations with lower frustration, aiming to move closer to others. This frustration, determined by propensity and distance, is crucial in shaping the system's dynamics. Given a nation *i*, with a configuration *X*, its frustration is:

$$F_i(X) = \sum_{j \neq i} s_i p_{ij} d_{ij}(X) \tag{2.1}$$

The weighted frustration formula accounts for agent size s_j, emphasizing collaboration with significant agents and maintaining the myopic assumption through pairwise evaluations. A configuration's energy (*E*) is the sum of individual frustrations.

$$E(X) = \sum_i s_i F_i(X) \tag{2.2}$$

$$E(X) = \sum_{i,j} s_i s_j p_{ij} d_{ij}(X) \tag{2.3}$$

In the context of agent collaboration, the energy and configuration are optimized, resulting in lower values than when agents operate in opposition. This relationship gives rise to an energy landscape representing configurations and their corresponding energies. A decrease in a single nation's frustration signifies a reduction in the system's overall energy. The energy transitions from a higher state to a lower one, stabilizing at a local minimum. According to the landscape theory[13], the system's configuration changes like a downhill movement, with stable configurations located at local minima. The theory also posits that symmetric propensities prevent the system from entering cyclic configurations.

It is important to note that achieving equilibrium does not necessarily mean reaching a global minimum. The system's evolution is influenced by its initial conditions and history, causing it to settle in a corresponding basin rather than the lowest energy or frustration state. In essence, the landscape theory leverages propensity and size to calculate configuration energy, providing predictive insights into the system's behavior.

2.5 Axelrod's Tribute and Conflict Model

In this we present the fundamental theory that constitutes the basis for the present Thesis. The prominent social scientist Robert Axelrod proposed an ABM model to explore the intricate processes where agents sacrifice some autonomy for more efficient collective organization. In an famous article, entitled "Building new political agents"[7], Axelrod investigates how larger political entities arise from interactions among smaller ones. He establishes criteria to identify emerging political agents: effective control over subordinates, collective action, and recognition by others. This model can be applied to diverse situations that involve power relations, from the rise of empires, mafia organizations, conflicts among nations, the dynamics of warfare, to personal relations and negotiations.

At the heart of the model lies a "pay or else" dynamics inspired by the concept of extortion, a process Axelrod identifies as crucial in the formation of states or power organizations. The tribute model involves agents extracting resources through forced transfers known as tribute payments. This process empowers the extracting agent's status and weakens the payer's influence. Unlike territorial conquest, which is excluded from this model, the tribute model allows for future coordinated actions, sustaining the involvement of independent agents in the dynamics over time.

It is essential to understand clearly the symbols and notations that we shall use throughout this work. Table 2.1 below provides a comprehensive guide to the various symbols employed in mathematical expressions, models, and conceptual frameworks.

Table 2.1: Symbol Definitions

Symbol	Definition
N	Number of agents
W_i	resources of agent/coalition i
r	Harvest
q	Tribute amount
k	Constant of damage $[0, 1]$
λ	Activations per cycle year
τ	Target Coalition
α	Attacking Coalition
$V_{i,j}$	Vulnerability of agent j to agent i
C_{ij}	Commitment level between agents i and j

In the original formulation by Axelrod, the model employed a a set of N=10 independent agents distributed linearly with periodic boundary conditions to avoid introducing distinctions for agents at the border (see Figure 2.5(a). At that time, Axelrod lacked the computational resources for studying his theoretical ideas on a larger scale nor in other lattices.

In this Thesis, we implement Axelrod's model in a general form and on any network of connectivity. Our interest in exploring different topologies led to adopting a more realistic 2-dimensional lattice with periodic boundary conditions and a von Neumann neighborhood, as depicted in Figure 2.5(b). This transition impacts the scalability of

simulations, time, and complexity but introduces more realism to the systems under exploration. We also investigate Axelrod's model on a fully connected network to reflect our current globalized world.
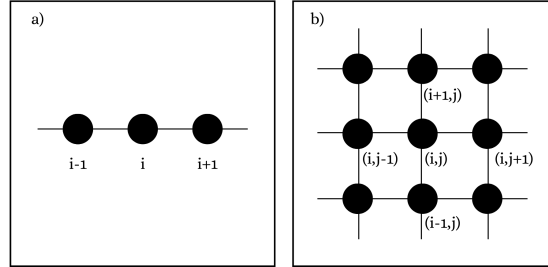

Figure 2.5: **Spatial Interaction:** a) 1D line with periodic boundary conditions. b) 2D square lattice with periodic boundary conditions and von Neumann neighborhood.

In the model, agents are represented as nodes on a lattice or network. Each agent i on the lattice is assigned an amount of wealth or *resources*, W_i, selected from a random distribution $W_i \in [W_{min}, W_{max}]$.

In each simulated year, ambitious leaders emerge randomly, targeting 30% of the total agents to demand tribute from one of their neighbors. This condition is initially imposed, but contiguity requirements are relaxed as alliances form, allowing for more flexible dynamics. However, the contiguity of commitments remains crucial to preserve the dynamics of land combat.

When presented with the opportunity to make a demand, agent A can initiate a demand to an agent I if it is currently favorable. If the demand is made, agent T will "fight if and only if it would cause less damage than paying would."[7] The ensuing dynamics lead to the following outcomes:

- **T pays tribute:** The transfer of resources occurs from T to A. If the total resources of T, denoted as W_T exceed the tribute amount q, then the transferred quantity is q, otherwise, T transfers its entire resources to A

- **T fights rather than pay:** In this scenario, each side incurs losses proportional to the resources of its opponent, and the losses are defined by:

$$L_A = kW_T \tag{2.4}$$

$$L_T = kW_A \tag{2.5}$$

where k is a constant of damage.

It is important to note that both sides incur in losses, but the stronger side is affected more significantly than the weaker side.

The current model is out of equilibrium, where each conflict depletes the system's resources, behaving as a dissipative system. To counteract this, after each yearly cycle, resources are reinjected into the system by augmenting the resources of each agent by an amount r.

Within the extortion framework, agent A must strategically select a target that strikes a delicate balance—being weak enough to choose payment over resistance yet strong enough to offer a substantial contribution. For this reason, a quantifiable measure, referred to as the vulnerability of agent j with respect to agent A is defined as:

$$V_{A,j} = \frac{W_A - W_j}{W_A} \tag{2.6}$$

We introduce susceptibility S as a metric for optimal target selection. This metric incorporates both the vulnerability of the target agent and its ability to pay tribute. The susceptibility S_j of agent j is calculated as follows:

$$S_j = V_{A,j} \times \min(W_j, q) \tag{2.7}$$

The function $min(W_j, q)$ ensures that the ability to pay does not exceed the tribute value q. After calculating the susceptibility S_j for each agent j, we select the agent that has the highest susceptibility among all possible agents. This means we select the agent that is most vulnerable and has the highest ability to pay.

If there is no potential target weaker than the demander (i.e., there is no agent j for which $S_j > 0$), no demand is made. Conversely, agent j engages in a fight only if $L_j < \min(W_j, q)$.

Transitioning from metrics for target selection, let us delve into how agents coordinate actions in the model. The primary mechanism for this coordination is establishing commitments among agents, influencing their future decisions within the conflict dynamics. Subject to incremental adjustments, these commitments play a pivotal role in shaping agent behavior in response to conflicts, whether paying tribute or engaging in a fight. The commitment dynamics are represented by a symmetric matrix of dimensions $N \times N$. To initiate this process, the commitment matrix is initially defined as follows:

$$C = \begin{bmatrix} 1 & 0 & \dots & 0 \\ 0 & 1 & \dots & 0 \\ \vdots & \vdots & \ddots & \vdots \\ 0 & 0 & \dots & 1 \end{bmatrix} \tag{2.8}$$

Each agent is inherently committed to itself ($C_{ii} = 1$), while no commitments exist between distinct agents i and j initially ($C_{ij} = 0$). The visual representation of the initialized commitment matrix and the corresponding network is depicted in Figure 2.6. As time progresses, new connections are established, and the network undergoes dynamic changes reflecting the evolving commitments among agents.

The commitment level undergoes changes based on certain interactions. It increases in scenarios involving the transfer of resources from i to j (subservience) or from j to i (protection), as well as when both i and j engage in fights on both sides. Conversely, a decrease in commitment occurs when i exhibits hostility by fighting against j.

In explaining the coalition formation process within this model, we consider an adjacent agent, denoted as κ, which will align itself with the attacking coalition α under the condition $C_{A\kappa} > C_{T\kappa}$. Conversely, it will affiliate with the target coalition τ if $C_{A\kappa} < C_{T\kappa}$. In the event that $C_{A\kappa} = C_{T\kappa}$, agent κ maintains neutrality. As indicated earlier, the contiguity to demand rule is relaxed through coalition formation.

Figure 2.7 illustrates two coalitions formed along a 1D line for simplicity. For instance, if agent 1 aims to demand resources from agent 4, agents 2 and 3 must exhibit a higher level of commitment to agent 1 than agent 4. In a
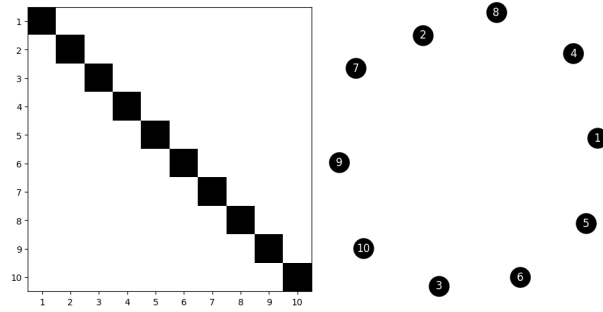
Figure 2.6: **Commitments Representations:** a) Initial commitment matrix for 10 agents, and b) corresponding network representation.
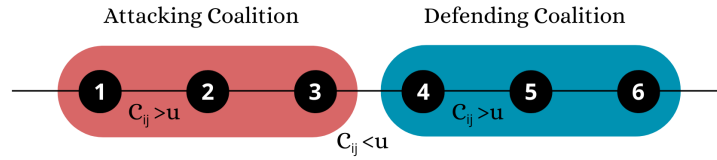
Figure 2.7: **Spatial Contiguity Restriction:** coalition formation

2D lattice, this alliance structure becomes more intricate, as each potential target must have multiple paths, thereby intensifying the maximization process of susceptibility. Agents pool their resources by aligning with a coalition and contributing proportionately to their commitment levels with the demanded or targeted agent. Consequently, coalition resources are defined as:

$$W_\alpha = \sum_{i=1}^{N_\alpha} C_{Ai} W_i \tag{2.9}$$

$$W_\tau = \sum_{i=1}^{N_\tau} C_{Ti} W_i \tag{2.10}$$

Where N_α and N_τ are the number of attacking and target coalitions elements. When assessing vulnerability within existing coalitions, commitments and resources are treated as common knowledge. Subsequently, the model considers potential coalition formations for each target agent.

$$V_{Ai} = \frac{W_\alpha - W_\tau}{W_\alpha} \tag{2.11}$$

In determining conflict losses, the model distributes these losses proportionally among the contributors within the coalition. This allocation method ensures fair consequences sharing, emphasizing the collaborative nature of

coalition responses to conflicts. As before, the losses are defined as:

$$L_{i \in \alpha} = k W_\tau \frac{C_{iA} \times W_i}{W_\alpha} \qquad (2.12)$$

$$L_{i \in \tau} = k W_\alpha \frac{C_{iT} \times W_i}{W_\tau} \qquad (2.13)$$

The model constitutes a spatio-temporal dynamic system characterized by continuous states, discrete space, and time. It operates out of equilibrium, featuring coevolution where connections depend on local states and vice versa. In this dynamic environment, agents continually develop and establish commitments with one another based on their past interactions.

Importantly, the model is not grounded in rational decision-making, as Axelrod recognizes the inherent complexity that renders such calculations virtually impossible in this setting. However, despite its departure from strict rationality, the model, built on a few foundational assumptions, reveals intriguing phenomena. It holds significant value for studying self-organization, emergence, and other compelling dynamics with applications in political, economic, and population studies.

Chapter 3

Implementation of Axelrod's model on a 2-Dimensional Square Lattice

Axelrod's Tribute Model is relevant in the context of theories of conflicts and the formation of coalitions. However, to our knowledge, Axelrod's Tribute Model has not been computationally implemented on a full scale. In this Chapter, we implement the Tribute Model in a system of N agents on a 2-dimensional lattice with periodic boundary conditions, adopting a von Neumann neighborhood. Initially, each agent i in the lattice is assigned resources W_i selected from a uniform random distribution. The dynamics is driven by a fixed number of activations per cycle year λ, a yearly constant harvest r reinjected consistently for each agent, modifications to commitments c, a "destructiveness" constant k quantifying damage inflicted by opponents, and a demanded tribute q. The specific values for these parameters are outlined in Table 3.

Parameter	Value
N	100
W_i	[300, 500]
λ	33
r	20
c	10%
k	0.25
q	250

Table 3.1: Standard Tribute Model Parameters

Given the inherently stochastic nature of societal behavior, examining individual data to clarify the dynamics over the years is essential. The tribute model was run 50 times, each spanning 1000 cycle years (with 33 iterations corresponding to one cycle year), generating diverse populations under these conditions. Diversity arises from

the random selection of ambitious leaders and initial resource allocation, contributing to distinct trajectories in the simulated populations.

3.1 Non-Trivial Collective Behaviours

Selected for a focused case study, Figures 3.1, 3.2, and 3.3 represent distinct aspects over time for three random populations. In Plot (a), black lines indicate conflict events, and gaps represent periods of low conflict among agents. Plot (b) illustrates the total resources within each population, displaying dynamic fluctuations. Plot (c) utilizes a raster plot to depict individual agent resources, with varying intensities denoting levels relative to the global resources.

Figure 3.1: **Dynamics of Conflict and Resource Distribution for population 1:** Temporal patterns of conflicts occurrences (a), global resource availability (b), and individual agent's resource levels in a 2D square lattice. Peaks in conflict frequency links between resource scarcity/abundance and societal tensions. Parameters are as described in Table 3.

Analyzing the first population (Figure 3.1), Plot (a) showcases elevated conflict frequencies during initial iterations, around time 15000, and towards the final years. The former may be attributed to emergent system structuring and limited commitments, leading to targets finding attackers not as strong as they would be in a coalition. Plot (b) reveals that during the first 20000 iterations, global resources experienced slow growth, restricting the population to a maximum value of approximately 150000 (a.u.). This period aligns with the conflict occurrences. After this period, resources significantly increased despite localized conflict occurrences, reaching around 300000 (a.u.) towards the

simulation's end, followed by a substantial decrease.

In Plot (c), the raster plot shows a dynamic reshuffling of powerful agents accumulating resources, corresponding to high-frequency conflict periods outlined in Figure3.1(a). Initially, resource distribution is relatively equitable, but frequent conflict intervals deplete the system of resources. Consequently, the number of powerful agents diminishes, giving rise to a restructuring of relative power dynamics. This restructuring becomes evident at time 10000 and 31000 in Figure3.1(c). The abrupt shifts in global resources and restructuring of power agents suggest the occurrence of conflicts akin to "world wars."

Moving to the following example, we examine the historical dynamics of our second population (Figure 3.2). Plot a) suggests that conflicts occur more frequently and are more evenly distributed across time than the first population. Plot b) shows a significant increase in resources towards the end of the timeline, reaching a peak of approximately 400000 (a.u.). However, the resources remained at very low levels during the first 10000 time units (around 300 years). This could suggest a period of economic stagnation or resource scarcity, which might have contributed to the high frequency of conflicts observed in Figure3.2(a) during this period.
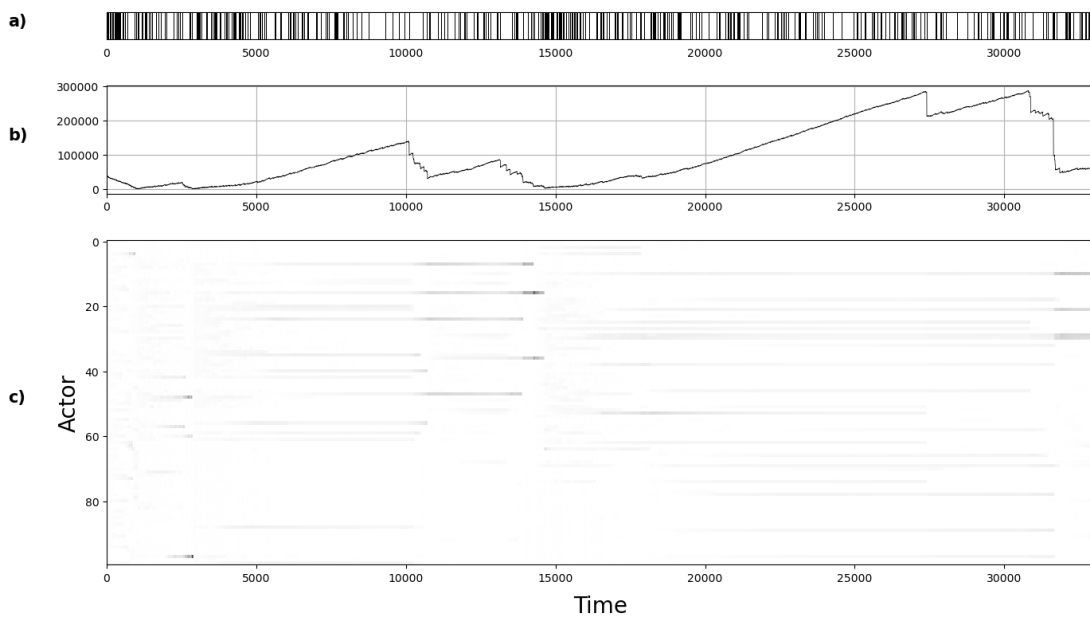

Figure 3.2: **Dynamics of Conflict and Resource Distribution for population 2:** Temporal patterns of conflicts occurrences (a), global resource availability (b), and individual agent's resource levels in a 2D square lattice. Resource scarcity triggers conflicts and concentration, while abundance facilitates equitable distribution and emergence of new powerful agents. Parameters are as described in Table 3.

In Plot c), initially, resources were more evenly distributed among the agents. However, during the period of economic stagnation, a few agents began accumulating more resources, resulting in a more unequal distribution. This distribution could have fueled tensions and conflicts within the population. The transition to an upward trend in

global resources might be due to the accumulation of conflicts among powerful agents, diminishing their strengths and allowing other agents to emerge. This phenomenon is evident around time 10000 in Figure3.2(c), where a new order of powerful agents appears. Periods of resource scarcity align with high-frequency occurrences of conflicts and a concentration of resources among a select few agents. Conversely, during periods of resource abundance, a more equitable distribution of resources is observed, facilitating the emergence of new powerful agents.

Our final analysis focuses on the third population (Figure 3.3). In plot a), we observe increased conflicts during the early years and approximately from 20000 onwards. Notably, the most drastic reductions in global resources do not coincide with the highest accumulation of conflicts. In plot b), this population's resources began to surge quickly without significant losses due to conflicts, peaking at approximately 300000 (a.u.) around iteration 12000. However, the global economy experienced a considerable decline in the subsequent years and maintained lower values. This period of stagnant resource growth aligns with the increased frequency of conflicts. In plot c), we note how decreases reduce the number of powerful agents, as evident in 3.3(c) at times 12500, 20000, 26000, and 30000.
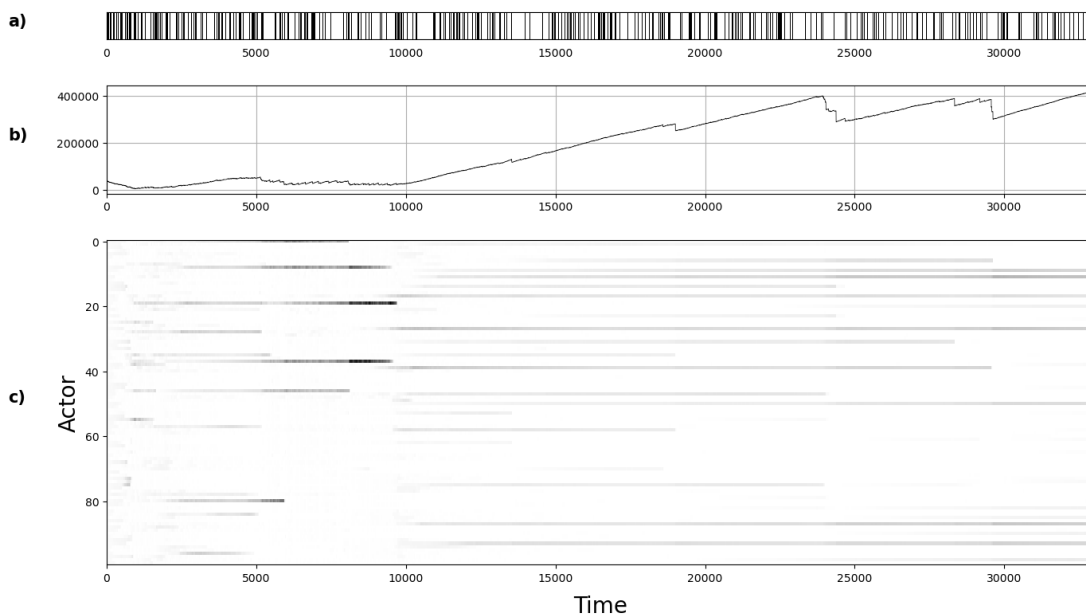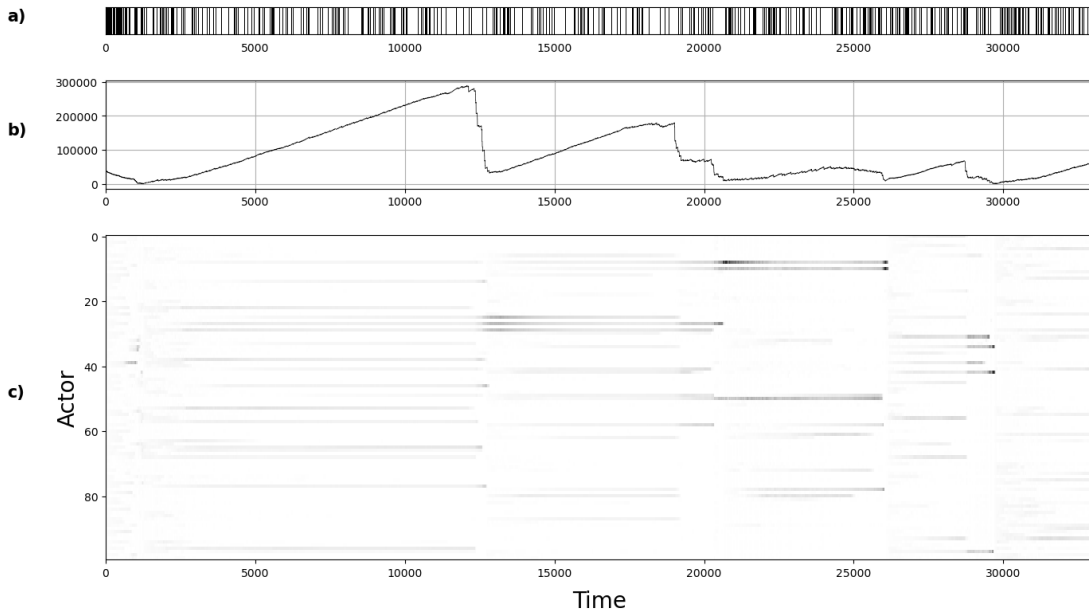

Figure 3.3: **Dynamics of Conflict and Resource Distribution for population 3:** Temporal patterns of conflicts occurrences (a), global resource availability (b), and individual agent's resource levels in a 2D square lattice. The accumulation of conflict frequency does not guarantee an immediate slump in the global economy. Parameters are as described in Table 3.

To summarize, each population has its unique trajectory, but there are common dynamics that can be identified. Initially, all populations experience a high degree of conflict. This could be attributed to the initial resources distribution w_i, the value of the tribute q, the absence of robust coalition formations, or a combination. In other words, it is more profitable for target agents to fight than to pay, leading to conflicts. However, as time progresses, the

formation of complex coalitions can prevent severe collapses, although exceptions may occur in the form of global wars causing significant economic slumps.

In other scenarios, the general trend is toward economic growth, mirroring the dynamics of a conflict-free environment where resources are transferred and agents harvested annually, leading to an increase in the global economy. The plots reveal that resource inequality fluctuates over time, with some agents possessing more resources than others.

It is important to note that a high frequency of conflicts does not necessarily guarantee a sharp decline in the global economy. Instead, these conflicts may serve as a mechanism for restructuring commitments within and between coalitions. This mechanism can draw powerful agents into future conflicts, allowing new powerful agents to emerge gradually.

Motivated by this mechanism, we explore the nature of conflicts. We examine a 500-cycle years after a transitional period of 500 years, showing significant findings on conflict patterns. Table 3.1 provides a statistical overview of conflict distributions, indicating the types of conflicts (civil wars and non-civil) that amount to 825000 cases. Civil wars are defined as conflicts where the attacker and the target are at least 50% committed.

	Total	Mean	Median	Mode	Standard Deviation	Skewness	Kurtosis
Conflicts	196529	7.9	8.0	8	3.4	0.35	0.02
Civil wars	168249	6.7	6.0	5	3.2	0.50	0.20
Non-Civil	28280	1.1	1.0	0	1.2	1.42	2.87

Table 3.2: Summary Statistics of Conflicts Nature (Civil and Non-Civil Wars) for a cycle year in a 2D square lattice.

We recorded a total of 196529 conflicts. These conflicts exhibit moderate variability with a standard deviation of 3.4. The distribution is slightly right-skewed, as indicated by the skewness value of 0.35, and is relatively normal due to the low kurtosis value of 0.02.

Civil wars constituted a significant portion of these conflicts, with 168249 occurrences. This conflict accounts for approximately 86% of all recorded disputes. The distribution for civil wars is also slightly right-skewed with a skewness value of 0.50 and has relatively light tails, as suggested by the kurtosis value (0.20). This skewness is confirmed by having a higher mean (6.7) than both median (6) and mode (5).

On the other hand, non-civil wars accounted for 28280 instances during this time frame, which translates to an average occurrence rate of about 1.1 per year; however, there was moderate variability in their annual occurrence as indicated by the standard deviation (1.21). The distribution for non-civil wars was strongly right-skewed with a skewness value (1.42), indicating that some years experienced significantly higher numbers than others; this observation is further supported by high kurtosis (2.87), suggesting heavy tails in the distribution.

Indeed, these statistical insights provide an intricate understanding of the nature of conflicts on this lattice model; civil wars were more prevalent, but non-civil wars showed more substantial variability and extreme values than civil wars. Nevertheless, it is also worth investigating any recurrent and discernible patterns in size distribution or the number of agents involved, particularly in dynamics that propel societies toward internal strife.

We analyzed the empirical data from 50 population realizations over a 500-year transient period and found that

the distribution of the number of agents involved in conflicts has heavy tails. Therefore, we used the Python package *powerlaw* [16] to examine the heavy tail distributions. Figure 3.4 shows the Complementary Cumulative distribution with two candidate models: a power-law fit and a truncated power-law fit. Power-laws are heavy-tailed probability distributions defined as:

$$P(x) \propto x^{-\alpha}$$

where α is the power-law exponent. On the other hand, a truncated power-law consists of a power-law truncated by an exponential part defined as:

$$P(x) \propto \alpha x^{-(\alpha+1)} e^{-\lambda x}$$

where α is the power-law exponent and λ the exponential part.
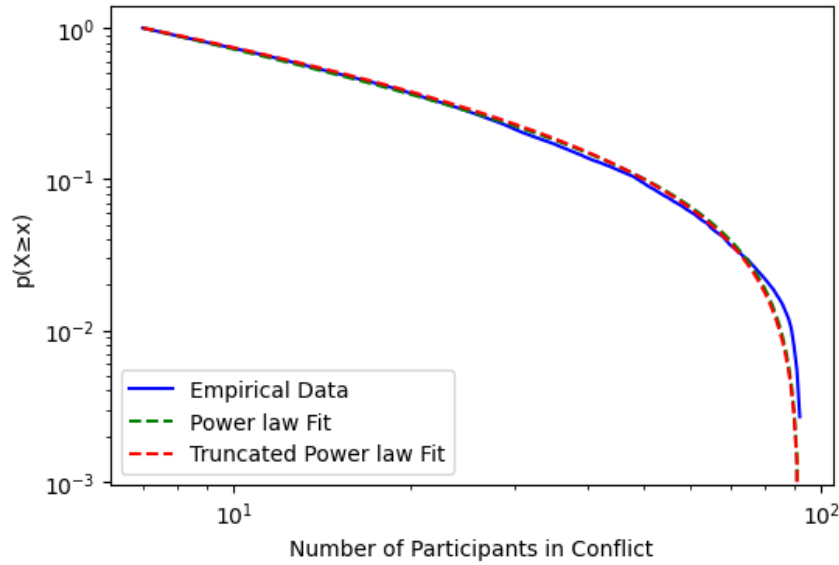
Figure 3.4: Complementary cumulative distribution functions of the number of participants in conflicts and fitted distributions, with an upper limit (*xmax* = 92)

Some distributions have an upper limit due to finite-size scaling or theoretical limits, preventing data from going beyond [16]. We set an upper limit of *xmin* = 92 based on visual data inspection. We noticed that the CCDF of data in Figure 3.4 bends down because of the nature of cumulative functions reaching this upper limit.

We performed a goodness-of-fit test under these two different distributions. The loglikelihood ratio returned a value of −13.62. This negative value suggests that the data is more likely under the second distribution (Truncated power-law). The p-value of the likelihood ratio test of 0.0 suggests that the likelihood difference is statistically significant. This result suggests that the data is better fitted with a power law (α = 1.57) exponentially truncated(λ = 0.01).

In essence, the participation of few agents in conflict is more probable. It could be due to the high and dense commitments within coalitions that make the strongest agents act indifferently, resulting in more civil wars. In

contrast, global wars are rare (involving most of the lattice participants) because conflicts between coalitions might not be economically optimal or beneficial.

In the context of economic dynamics, understanding the distribution of global resources over time is crucial for assessing the fairness of goods. We use the Gini index, a widely used indicator of resource distribution in a population. The Gini index ranges from 0 to 1, where 0 means perfect equality and 1 means perfect inequality, where one agent has all the resources. We apply the formula given by Herrera et al.[17] to calculate the Gini index:

$$G(t) = \frac{\sum_{i,j=1}^{N} \left| w_i(t) - w_j(t) \right|}{(2N) \sum_{i=1}^{N} w_i(t)} \tag{3.1}$$

Figure 3.5(c) shows the index fluctuations over time in population 1. We can see how conflicts lead to inequality. Despite the volatility periods, the index tends to stabilize near 0.85, which is a high value, indicating that this model generates high inequality.
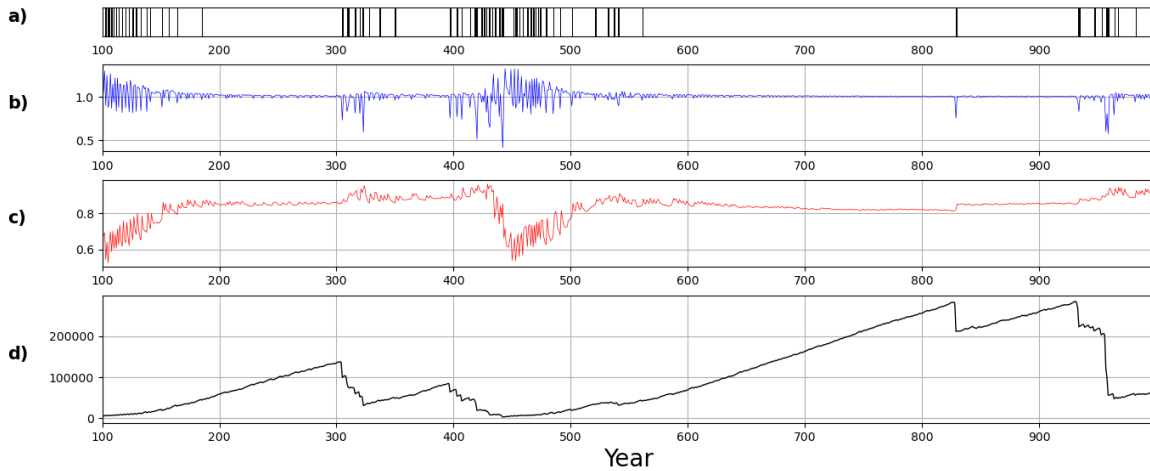
Figure 3.5: **Global Resource Dynamics and Conflicts in Population 1:** The figure shows four plots representing data on global resources and conflicts over 900 years. Plot a) shows the frequency of conflicts with a significant impact on global resources, b) the Ratio of consecutive global resources, c) the Gini index, and d) the Dynamics of global resources.

As we stated before, conflicts cause a redistribution of resources, but we observe that not all high-frequency conflict periods have immediate effects. We focus on those severely affecting global resources to identify extreme violent conflicts. We start by computing the ratios of consecutive global resources and then calculate the interquartile range (IQR) excluding the first 100 years. The threshold is set as 1.5 times the IQR. Values below this threshold from the lower quartile are considered outliers, as we are only interested in resource losses. Figure 3.5(a) illustrates the frequency of outlier conflicts, and Figure 3.5(b) shows the ratio of consecutive global resources. We notice the correlation between the variations of the Gini index and the occurrence of violent conflicts.

As depicted in Figure 3.5(a), certain activities demonstrate a temporal process that is not uniform. These activities are characterized by periods of high activity interspersed with periods of low activity[18]. This pattern results in a fat-tailed distribution of inter-event times, a phenomenon observed in both non-violent[19] and violent human activities[20,21]. This pattern is referred to as bursty behavior.

Barabasi[22] proposed that this bursty behavior is a consequence of a decision-based queuing process. The timing exhibits a heavy tail when tasks are executed based on priority. This allows for extended periods of inactivity, punctuated by bursts of intense activity. Similar patterns have been observed in the distribution of inter-event times in natural phenomena such as earthquakes[23] and fracture experiments[24].

However, it is essential to note that different generative mechanisms can yield different distributions. The focus should be on something other than whether the data adheres to a specific distribution; instead, it should focus on identifying the most suitable model for the situation. For instance, it has been argued that a log-normal distribution provides a more accurate and appropriate description of human communication, contrary to Barabasi's analysis[25].

While a power-law distribution may arise from preferential attachment or optimization mechanisms, a log-normal distribution results from a multiplicative process; a random variable x is said to be lognormally distributed if the random variable $Y = lnX$ follows a normal distribution with mean μ and standard deviation σ. The density function is given by:

$$f(x) = \frac{1}{\sqrt{2\pi}\sigma x}e^{-(\ln x - \mu)^2/2\sigma^2} \tag{3.2}$$

Despite the log-normal distribution having finite moments and the Pareto distribution having infinite moments, their plot shapes are remarkably similar, with a large portion of the body of the density function and the complementary cumulative distribution function appearing linear.

The tribute model, while not intended to be a detailed representation of reality, serves to identify common characteristics of social dynamics. Figure 3.6 presents the probability density function of the inter-event time distribution between violent conflicts, comparing a log-normal distribution and a power law distribution.
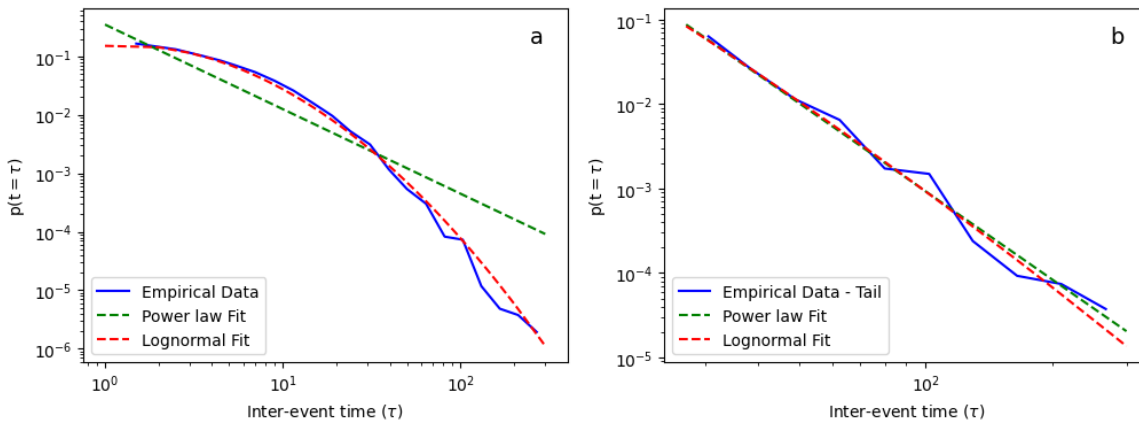

Figure 3.6: PDF of the inter-event times between violent conflict and fitted distributions, for a) all regime , and b) for the tail (*xmin* = 27).

Table 3.1 presents the results of a goodness-of-fit for all the data and the tail. The test compares distributions returning the loglikelihood ratio and the p-value for the pair of distributions.

Regime	Distributions	loglikelihood ratio	p-value
xmin = 1 xmax = None	Log-normal/Power law	62.11	0.00
xmin = 27	Log-normal/Power law	0.79	0.43

Table 3.3: Goodness-of-Fit test for inter-event time distribution considering a Log-normal and a power law fit.

From Table 3.1, it is observed that for *xmin* = 1, the log-likelihood ratio is 62.11 with a p-value of 0.00, indicating a significant difference in fit quality favoring the log-normal distribution over the power law. For *xmin* = 27, however, this ratio drops to 0.79 with a p-value of 0.43, suggesting no significant difference between the two fits. The fitted parameters for the log-normal distribution are $\mu = -3.43$ and $\sigma = 1.73$ for all data and $\mu = 1.46$ and $\sigma = 1.13$ for data with *xmin* = 27. In terms of which distribution fits better, the log-likelihood ratio and p-value suggest that the log-normal distribution better fits the data when considering all regimes (*xmin* = 1). However, when focusing on the tail of the distribution (*xmin* = 27), there is no significant difference between the log-normal and power law fits.

In our analysis of the upper limit (tail), we estimate a power-law exponent of 3.47, which leads us to consider bursty patterns in financial interactions. These interactions, which include trades in futures markets, stocks, and foreign exchange, are primarily defined by transactions, so the inter-event time measures the interval between two consecutive transactions. These inter-event time distributions have been demonstrated to be heavy-tailed[26] and range from 1.3[19] to 3.47[27]. Our obtained value is at the end of this range. While we do not claim that the exact mechanisms governing financial trades also govern our empirical data, this observation might suggest potential mechanisms to clarify the generative model.

Meanwhile, Poissonian bursts offer an alternative description for individual bursty activity patterns, such as those studied in the inter-event time and waiting time distributions in email activity logs[28] showing a better approximation to log-normal distributions. The mechanism under consideration is based not on rational analysis but on the routine performance of activities. In the context of our model's generative mechanism, this could provide a better understanding of political tension when considering all the data.

Another possible alternative for fitting the data is a double Pareto distribution.It has been stated that an appropriate double Pareto distribution can closely match the body of a log-normal distribution and the tail of a Pareto distribution[29]. Double Pareto log-normal distributions have proven helpful in modeling distributions of various complex networks and natural phenomena, including computer networks, social networks, and economics[30,31]. This suggests that most inter-event times between violent conflicts are relatively small due to the log-normal part, but there are also some rare instances where the inter-event times are extremely large due to the power-law tail.

In summary, the optimal waiting time of agents might be driven by objectives such as maximizing profit or utility. This may lead to different burst patterns. The times are distributed so that most are relatively close together, but there are occasional "bursts" of significant times. This is indicative of bursty behavior. This could imply that violent

conflicts tend to occur in clusters, with periods of relative calm in between. Despite the variety of possible fits and generative models, we get valuable insights to understand the underlying processes better. However, it is essential to note that these models simplify reality, and we might find better fittings with more parameters.

3.2   Spatial Resource Distribution and Coalition Formation

Another perspective to explore the tribute's dynamics involves analyzing the evolution of commitment patterns, which significantly influence global resources. Initially, each member is committed to himself. However, as rules and interactions occur over time, the structure of commitments evolves, as illustrated in Figure 3.7 for *population 1*. As time progresses, identifying aggregations of agents becomes more challenging due to the increasing complexity of the commitment structure. To better visualize these dynamics, we generate a graph using snapshots of the commitment matrix. We construct an adjacency matrix by establishing weighted edges between nodes if their commitment reaches at least 50% of the total commitment. Once the graph is constructed, we employ the Louvain community detection algorithm via the *community.best_partition* module of *Python* to identify clusters. The resulting graphs provide a clearer view of the inter and intra-cluster connection dynamics and reveal an essential visualization of aggregated agent dynamics.

In the system's early years, commitments start to grow, but they do so locally. By year 10, the population presents few connections established and minimal neighboring relations. However, by year 50, we begin to see the aggregations of agents emerge. By year 100, the network has evolved into two distinct clusters with no interconnections. These clusters persist in the following years, exhibiting variations in their internal connections. They either become more densely connected among themselves or show fewer intra-cluster connections.

Using commitment network visualization significantly simplifies identifying emergent aggregate agents compared to relying solely on matrix visualization. However, the matrix approach should be considered as it can offer valuable insights, particularly regarding the effects of the utilized topology.

We observe a tendency for commitments to grow locally within this topology. This pattern can be attributed to the inherent constraints of the system, which encourage agents to interact predominantly with their nearest neighbors. The reasoning behind this behavior might be rooted in optimization: more considerable distances and coalition sizes would entail a remarkable economic sacrifice, thereby rendering such interactions less profitable.

Our final interest is understanding how resources are distributed within coalitions, as this can provide insights into the observed behaviors. Figure 3.8 provides a visual representation of this distribution, showcasing the spatial allocation of resources (depicted as a heatmap) and the formation of coalitions (indicated by colored backgrounds) within a 2-D square lattice.

In the initial period, Figure 3.8 (a) corresponding to the first year, we observe an almost uniform distribution of resources among all agents, with no discernible cluster formation. However, as time progresses to years 300, 600, and 1000, represented by Figure 3.8 (b), (c), and (d), respectively, we begin to identify powerful agents who are more committed to each other, leading to the formation of a dominant aggregate agent or coalition over time. It is important to note that not all agents remain in the same cluster over time. The belonging of agents is dynamic, and a coalition can change in size and power.

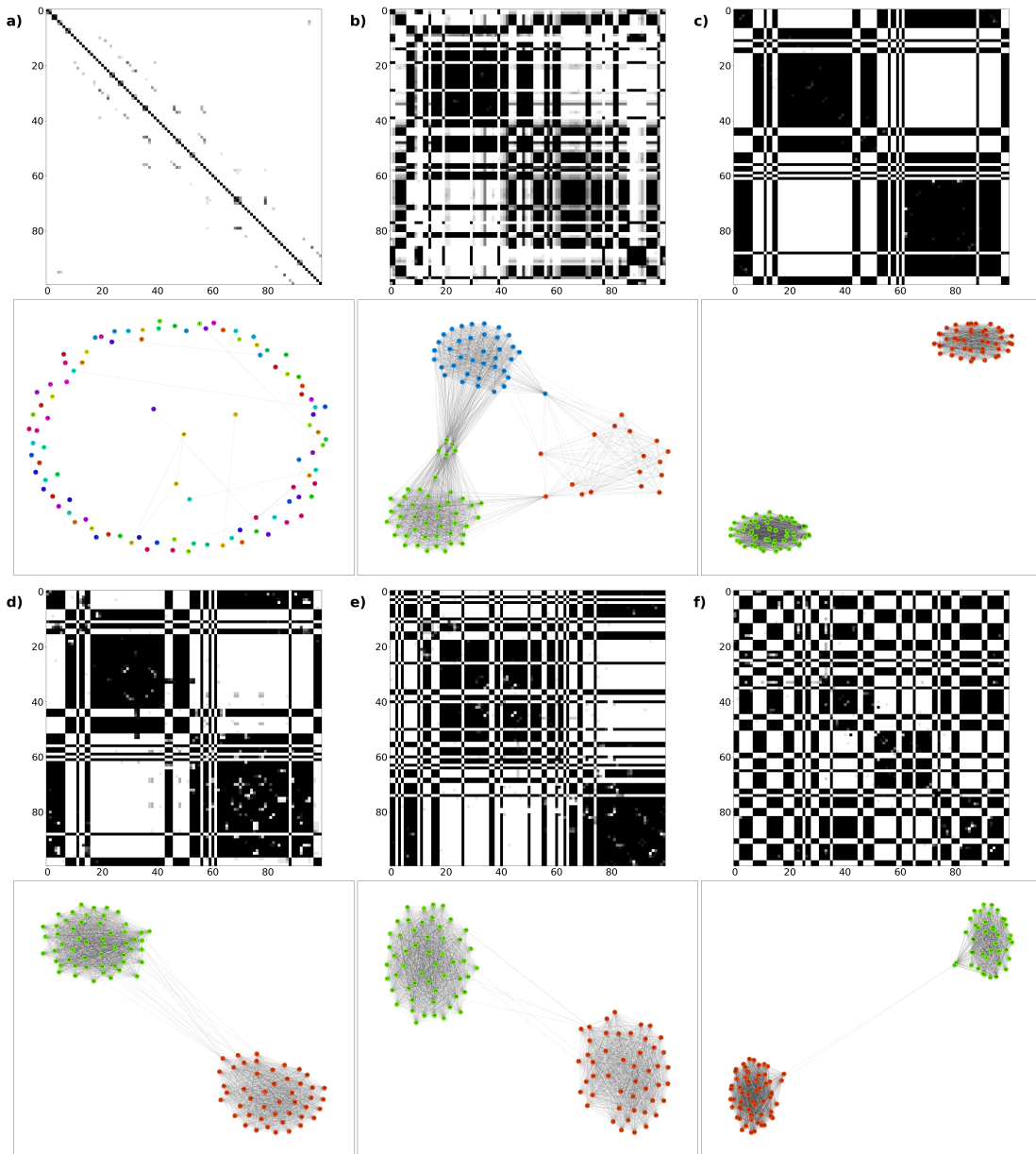Figure 3.7: **Commitment Patterns in a 2d Square Lattice:** The first row (a, b, c) illustrates commitment matrices at years 10, 50, and 100 with its corresponding graph below of the dynamics of population 1. In the second row (d, e, f) illustrates commitment matrices at years 200, 500, and 1000 with their corresponding network. We exclude commitment of agents falling below a 50% threshold. Parameters are as in Table 3.
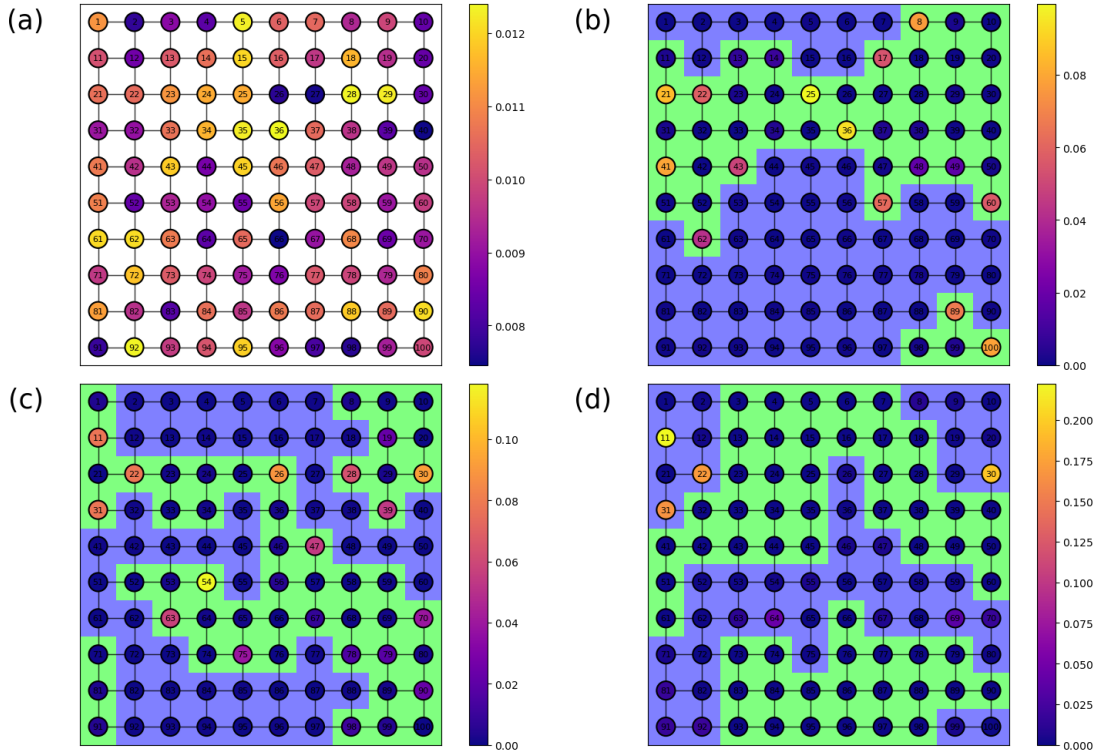
Figure 3.8: **Spatial Resources Allocation and Coalition Formation:** Population 1, N = 100, 2D square lattice with periodic boundary conditions. a) Resources distribution (heat map) at year 0. b) Resources distribution at year 300, where green and purple represent different clusters with members committed more than 50%, and more powerful agents form a single coalition. c) Resources distribution at year 600. d) Resources distribution at year 1000.

This behavior can be explained by considering extortion as a mechanism of resource accumulation. This mechanism allows powerful agents to maintain their status at the expense of weaker ones, limiting their attack opportunities. Therefore, more vulnerable agents must wait for the powerful agents to be weak enough to attack. One mechanism that might allow this is the disruption in internal coalitions and civil wars. Civil wars are necessary to weaken the power of the dominant aggregate agents by facilitating the restructuring of commitments and resources and providing an opportunity for others to emerge.

The Landscape Theory of Aggregation offers a plausible method to calculate the energy configuration of this system by considering the size of an agent as their resource and their propensity as commitments. To capture the essence of frustration within the system, we need to adjust the range of commitments. In this case, we can re-arrange the commitments from -1 to 1 to denote friendship or hostility, so frustration decreases within more committed agents. The final equation becomes:

$$E(X) = \sum_{i,j} w_i w_j c_{ij} d_{ij}(X) \tag{3.3}$$

Here, we use a binary representation of d_{ij} to denote group membership. As per the Landscape Theory, a system reduces its frustration and, consequently, its overall energy by transitioning to lower energy levels, resulting in more stable configurations. One way to reduce frustration is by increasing the resources of coalition members, as depicted in Figure 3.8. Presumably, the system's dynamics allow for exploratory configurations, aiming to reach local minimums. This analysis enhances the understanding of the system's behavior. Through this process, we can gain valuable insights into how agents interact and influence the system. Such insights can provide a foundation for informed decision-making and optimizing the overall energy state of system operations.

Chapter 4

Implementation of Axelrod's Model on a Global Network

The following compelling question concerns the effects of modifying the structure and connections of the distributed agents within the system. We propose an extreme case—a globally interconnected network to investigate this. Using identical parameters as those in the 2D square lattice scenario (see Table 3 for reference), we execute the model 50 times, resulting in 50 distinct populations. Interestingly, this new configuration tends to show a higher frequency of conflicts and a decrease in overall resources compared to the 2D square lattice configuration.

As an illustration case, Figure 4.1 shows a population characterized by frequent conflicts, low resource levels, and dynamic power structures. Figure 4.1(a) shows that the frequency of disputes appears to be evenly distributed, with many occurrences. Despite fluctuations, figure 4.1 (b) highlights that global resources remain within a narrow range. Despite disturbances, the resources tend to return to low values. Figure 4.1(c) shows that the distribution of powerful agents over time behaves similarly to a turbulent fluid. This distribution could be due to the low level of global resources, which prevents relative high accumulation of resources. Consequently, each agent frequently finds a profitable target, leading to a dynamic and unstable power structure.

Table 4 provides a comparative analysis of the conflict simulations performed on the two modeled network typologies: a 2D square network and a global network. The primary metrics analyzed are the Gini index and average global resources. We disregard an initial transient period of 500 years for each topology and calculate averages over the subsequent 500 years. This process is replicated across 50 populations, and the resulting values were averaged to yield the final values.

The Gini index for the 2D Square Lattice is 0.86, indicating a high level of inequality in resource distribution, and the standard deviation of the Gini index of 0.02 points to a moderate level of inequality variability among the different populations in this topology. On the other hand, the Gini for a global network is 0.72, implying a more equitable distribution of resources. The standard deviation for this case is lower at 0.01, showing a much lower variability across populations. This could be attributed to the interconnected nature of the global network facilitating resource flow across agents.
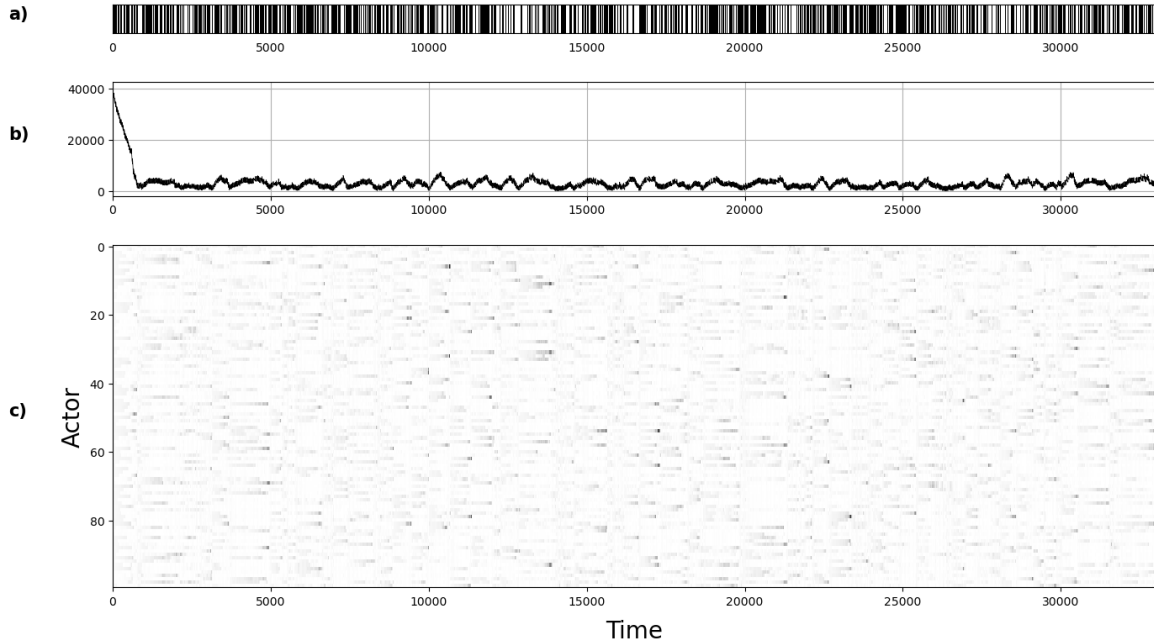
Figure 4.1: **Dynamics of Conflict and Resource Distribution in a Global Network for Population 1:** Temporal patterns of conflicts occurrences (a), global resource availability (b), and individual agent's resource levels in a global network. Population characterized by frequent conflicts, low resource levels, and dynamic power structures. Parameters are as described in Table 3.

Indeed, the high values of the Gini index observed in both structures can be explained by the inherent nature of the model, extortion. However, exploring how different strategies or policies could mitigate this effect and promote a more equitable distribution of resources would be interesting. While the 2D square grid shows greater inequality and variability, the global grid shows a more impartial and consistent distribution of resources.

As in the previous chapter, we also analyze the nature and distribution of conflicts in a global network over a cycle year. Table 4 summarizes the statistics of conflicts, both civil and non-civil wars, over a cycle year in a global network.

A total of 491,220 conflicts were recorded, with civil wars constituting a significant majority at 90% (444,188 occurrences). The standard deviation of 4, skewness (-0.05), and kurtosis(-0.23) values close to zero suggest moderate variability in the total number of conflicts and a relatively normal distribution.

Civil wars exhibit a slightly left-skewed distribution, as evidenced by their skewness value of -0.11, indicating that the data points concentrate on the right side of the distribution graph. This distribution is corroborated by mean, median, and mode values of 17.8, 18, and 17, respectively. A kurtosis value of -0.28 implies that the tails are less heavy than a normal distribution; thus, there are fewer extreme values.

In contrast, non-civil wars accounted for only 47,032 cases but exhibited strong right-skewness with a value of

	Gini index	σ (Gini)	Mean Global Resources
2D Square lattice	0.86	0.02	2.7×10^5
Global network	0.72	0.01	1.9×10^3

Table 4.1: **Comparative Analysis.** The data provide clarity on the differences observed between the two network models in terms of their impact on conflict dynamics.

	Total	Mean	Median	Mode	Standard Deviation	Skewness	Kurtosis
Conflicts	491220	19.6	20	20	4.0	-0.05	-0.23
Civil wars	444188	17.8	18	17	4.2	-0.11	-0.28
Non civil	47032	1.9	2	1	1.4	1.16	1.87

Table 4.2: **Conflicts Nature in a global network:** Summary Statistics of Conflicts Nature (Civil and Non-Civil Wars) for a cycle year.

1.16; this indicates an asymmetrical distribution where several years experienced significantly higher numbers than others, a scenario of sporadic intense conflicts. The kurtosis value stands at an elevated level (1.87), pointing towards heavier tails and, thus, more frequent extreme values in comparison to civil wars, while civil wars are more frequent but relatively consistent in occurrence across years; non-civil conflicts, though less frequent can be unpredictable and vary greatly in intensity from one year to another.

Following the same procedure as in Chapter 1, Figure 4.2 shows the CCDF of participants in conflict in a global network. It provides a statistical analysis comparing different probability distributions: the exponential law distribution, the truncated power law distribution, and the log-normal distribution. The upper limit has been established as *xmax* = 92.

Table 4 shows that for all comparisons, the p-values are 0.0, indicating that the differences between the distributions are highly significant. The loglikelihood ratios are also substantial, providing strong evidence for one distribution over another.

Regime	Distributions	loglikelihood ratio	p-value
xmin = 1	exponential/truncated power law	424.44	0.0
xmax = 92	log-normal/truncated power law	468.98	0.0
	log-normal/exponential	174.22	0.0

Table 4.3: Goodness-of-Fit of the number of participants in a Global Network

The exponential law distribution is more likely than the truncated power law distribution, as indicated by a loglikelihood ratio 424.44. Meanwhile, the log-normal distribution is more likely than the truncated power law distribution, with a loglikelihood ratio 468.98. Furthermore, the log-normal distribution is more likely than the
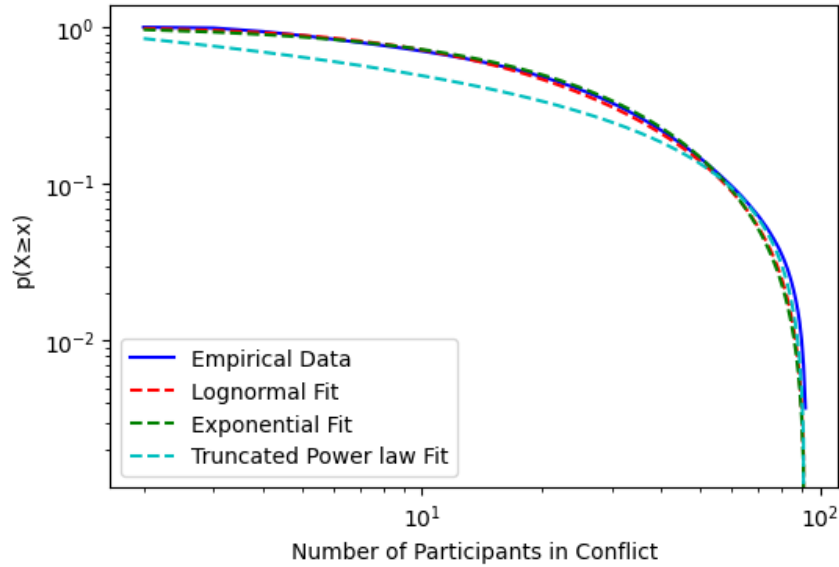
Figure 4.2: Complementary cumulative distribution functions of the number of participants in conflicts in a global network and fitted distributions, with an upper limit (*xmax* = 92)

exponential distribution, with a loglikelihood ratio 174.22.

The analysis indicates that the log-normal distribution is the most probable model, followed by the exponential distribution. The parameters for the fitted log-normal distribution are μ = 3.04 and σ = 1.14. We see that the change in the topology and hence spatial interactions produces that this distribution be better fitted with a log-normal than a power-law. In fact, Mitzenmacher[32] proposes that log-normal and power-law distributions are closely related, with log-normal distributions often emerging as viable alternatives to power-law distributions across various fields. This implies that minor variations in dynamics could influence the distribution. However, it remains a heavy-tailed distribution, albeit without the extreme cases often associated with power-law distributions.

As we did in case 2d, the next point of interest corresponds to violent conflicts. However, the high frequency of conflicts and low resources (refer to Figure 4.1) mean that the system does not present events of interest. Therefore, we move on to visualizing patterns and formations of commitments.

Figure 4.3 illustrates the evolution of the commitment network over time within a global network. Each panel (a), (b), and (c) represents different stages (years 5, 500, and 1000, respectively), showcasing an increase in complexity and globalization in the distribution of agents within the network.

In Figure 4.3(a), the commitment matrix at year 5 shows a sparse distribution of agent commitments, indicating a low level of connectivity among agents. This is corroborated by the corresponding graph below, which shows a low connection structure, suggesting that agents are less committed to each other in the early stages of the network formation, leading to fewer conflicts.

By year 500, as shown in Figure 4.3(b), the commitment matrix displays a complex pattern of connections
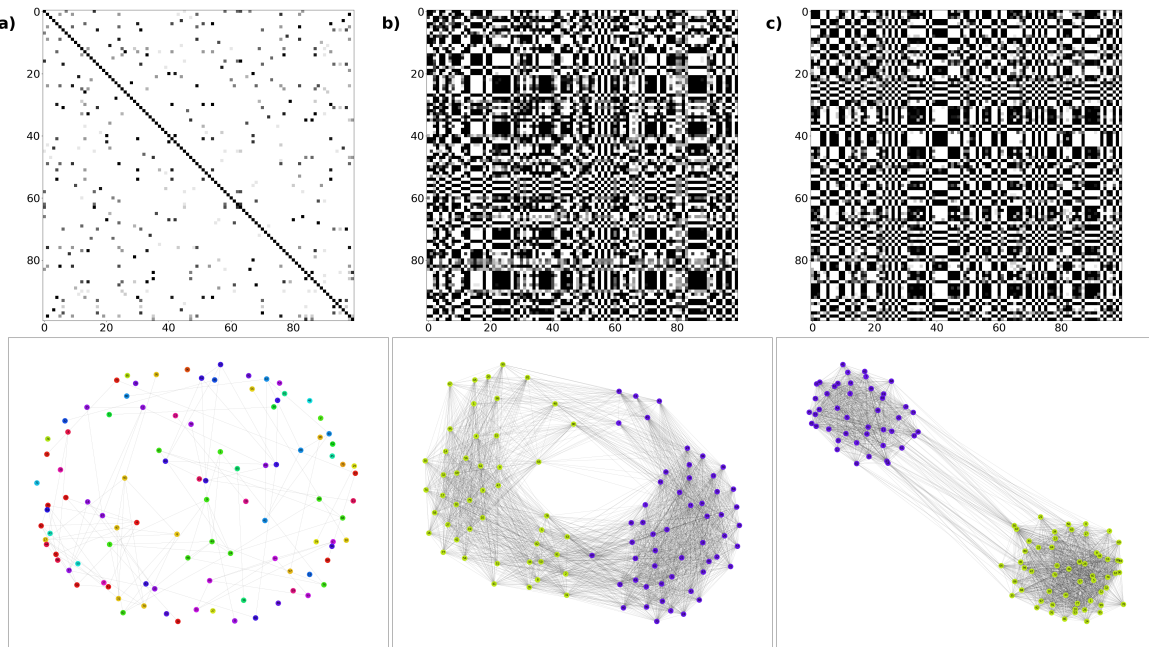
Figure 4.3: **Commitment Patterns in a Global Network:** Panels (a, b, c) illustrates commitment matrices at years 5, 500, and 1000 with its corresponding graph below of the dynamics of population 1. We exclude commitment of agents falling below a 50% threshold. Parameters are as in Table 3.

between the agents. The corresponding graph demonstrates increased complexity and connectivity in the network, indicating that over time, as agents form more commitments with each other, the network structure becomes more complex, potentially leading to more conflicts.

By the year 1000, shown in Figure 4.3(c), the complex pattern of connections continues, but the network's representation shows denser connections within clusters, with fewer connections to other clusters. Indeed, it suggests that, over time, agents form stronger commitments within their clusters, leading to a more stable network structure with fewer connections between clusters.

The transition from a 2D lattice to a global network moves from localized to more global interactions, where each agent has the potential to interact with any other agent in the network, regardless of its spatial proximity. This change has implications for the system's dynamics, including the rate and pattern of information propagation, as seen in the flow of resources.

While visual inspection provides limited success in discerning aggregate agent patterns in the commitment matrix, this task becomes increasingly challenging within the global network, emphasizing the importance of employing alternative visual methodologies, such as constructing an adaptive network of commitments, to understand better and interpret the complex interactions within the network.

Chapter 5

Simplified Target Selection in the Tribute Model: A Gateway to Phase Diagrams

This chapter arises from the need to explore strategies for mitigating the effects of conflicts and promoting equitable resource distribution. For this reason, we highlight the importance of constructing phase diagrams to understand the dynamics of the tribute model under different parameter variations. In identifying relevant parameters, we consider w_i and c to have a low influence on the system or be impractical. An advantageous initial resources allocation w_i does not guarantee success[7]. We also do not consider variations in commitment dynamics as we aim to keep it simple. For example, introducing a negative commitment could define enemies, but it would exceed our intentions.

On the other hand, we can merge the parameters λ and r into a single concept, which is the flux of resources periodically entering the system (r/λ). This new parameter is of interest since, without a periodic injection of resources, the dynamics of conflicts stop, leading to a single robust leader. Other important parameters are the destructiveness constant k and the tribute amount q, considered in the balance of participants' actions. N was not changed since the value used has already generated appreciable phenomena, and the scalability of the simulations would increase its running time. Even with this system size, we face the computational challenge of constructing phase diagrams on the 2D square lattice, as their simulation times are not feasible.

The most time-consuming aspect arises from target selection, which is more complex than it might initially appear. Based on the contiguity restriction, it requires an analysis and calculations of every possible coalition formation, which will define our final selection metrics. At early iteration times, the commitment matrix has not been significantly modified, and coalition analysis and target selection are faster, mostly just analyzing their neighbors or, less frequently, their second neighbors. However, as agents become more committed, the structure becomes more complicated. For a system of N agents, the attacker has to analyze $N - 1$ targets with their respective coalitions and then select the most beneficial one.

Our 2D square lattice model uses the Manhattan distance to calculate the minimum distance. This distance
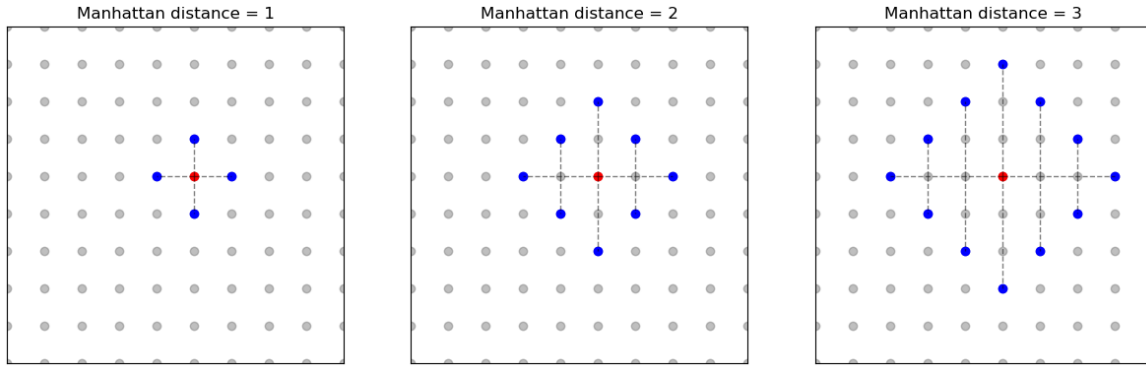
Figure 5.1: **Manhattan Distance.** Each subplot in the figure corresponds to a different Manhattan distance. The entire lattice is depicted using grey points. The central site is highlighted in red. Sites at specific distances from the central site are marked in blue. Dashed lines connect the central site to other sites, emphasizing the Manhattan distance between them.

defined for this grid-like space, between points $p_1(x_1, y_1)$ and $p_2(x_2, y_2)$ is:

$$\text{Manhattan distance} = |x_1 - x_2| + |y_1 - y_2| \tag{5.1}$$

In our 2D square lattice model, we employ the Manhattan distance to capture spatial interactions surrounding a specific lattice site (referred to as the "attacker"). The Manhattan distance measures the minimum number of lattice steps required to move from one site to another, considering only horizontal and vertical movements. Refer to Figure 5.1 for a visual representation of these distances within the lattice. The grey points represent the entire lattice. The central site is marked in red, while the sites at a certain distance are marked in blue. Each subplot in the figure represents a different Manhattan distance. In essence, we quantify the proximity of interacting agents by calculating the Manhattan distance. Chapter 1 (2D square lattice) provides empirical data to compute these distances.

The Probability Mass Function of these distances, shown in Figure 5.2(a), exhibits an intriguing exponential decay behavior. This pattern is fitted alongside the empirical data in the exact figure using a simple exponential decay model defined as:

$$p(x) = e^{-\gamma x}$$

The fitted parameter (γ) characterizes the decay rate of spatial interactions and was found to be 0.71. Refer to Figure 5.2(b) for the residual plot. This plot illustrates the differences between the observed order values and the values predicted by the exponential decay model, suggesting a good fit and reinforcing the reliability of the decay rate estimation.

Regarding modifications of the tribute model algorithm, for each ambitious leader (A), we select a single target based on an exponential decay probability (0.71) of distances covering all space in the lattice, thereby replicating the interactions of our 2D lattice. Once the target (T) is selected, we calculate its susceptibility $S = [V_{A,T} \times \min(W_\tau, q)]$ to determine if it is an optimal target ($S > 0$) to make the demand. It's important to note that this method eliminates
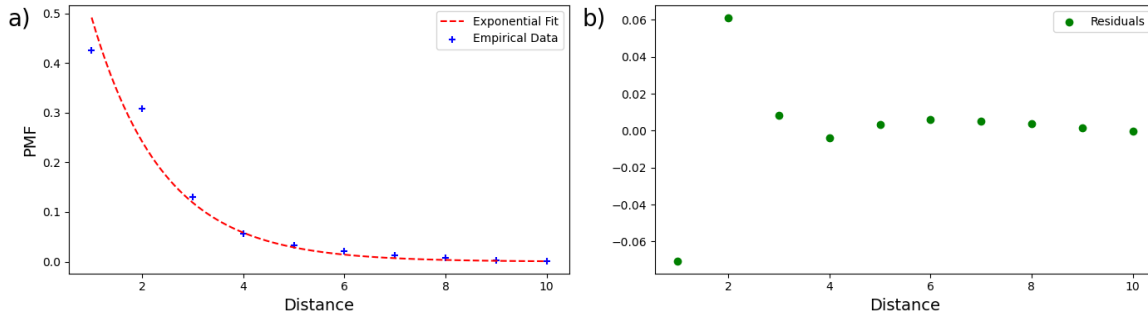
Figure 5.2: **Exponential Decay in Spatial Interactions.** The figure illustrates the empirical data from a 2D square lattice model (Chapter 1), showing the number of lattice steps away between attacker and target when conflicts occur. The Probability Mass Function (PMF) reveals an exponential decay pattern, fitted with a simple exponential decay model. The subplot (a) presents the PMF and the fitted model, while subplot (b) displays the residual plot, suggesting a good fit of the model to the actual data.

the contiguity restriction; hence, the coalition formation should not be restricted to spatial contiguity. From this point forward, the algorithm remains the same.

This approach allows for a flexible modeling of spatial interactions, emphasizing either local interactions (smaller distances) or global interactions (larger distances). Moreover, we reach a balance between capturing meaningful interactions and maintaining computational efficiency. The model remains computationally manageable while preserving the essential characteristics of the system.

To quantify the commitment activity between agents in the system, we use the following equation [17]:

$$A(t) = \frac{1}{(N-1)^2} \sum_{i,j} |C_{ij}^{t+1} - C_{ij}^t| \tag{5.2}$$

This equation provides a measure of how much the commitment matrix changes from time t to time $t+1$ by calculating the absolute difference between the elements of the matrix and then averaging these differences. Notably, conflicts induce more significant changes in the commitment matrix than tribute payments. This situation is primarily because conflicts, unlike tribute payments, are not confined to pair interactions but can involve multiple agents, leading to more substantial shifts in the commitment matrix.

In constructing accurate phase diagrams, it's crucial first to analyze specific metrics, such as the Gini index and the activity of the commitment matrix over time. This preliminary analysis aids in understanding how the system behaves under different parameters. Moreover, a temporal analysis ensures that the phase diagram captures not just static but dynamic behaviors, offering insights into system stability, transitions, and responses to parameter changes.

We begin by varying the destructiveness constant k, using values of 0, 0.25, 0.5, 0.57, and 1 over 200000-time steps, as shown in Figure 5.3. For each k value, the program was run five times, and the results were then averaged. For all variations of k, the Gini Index and the activity of the commitments show more significant variability and intensity during the first 100000 time steps. From this point onwards, for k values of 0, 0.5, 0.57, and 1, the Gini

index is relatively stable, and the activity of commitments presents low intensities over time. Except for $k = 0$, all the systems are highly unequal (high Gini index). However, $k = 0.25$ still presents fluctuations in the Gini index at a window of high values, indicating more dispersion but also high inequality of resources, and the activity of commitments still presents high intensities.
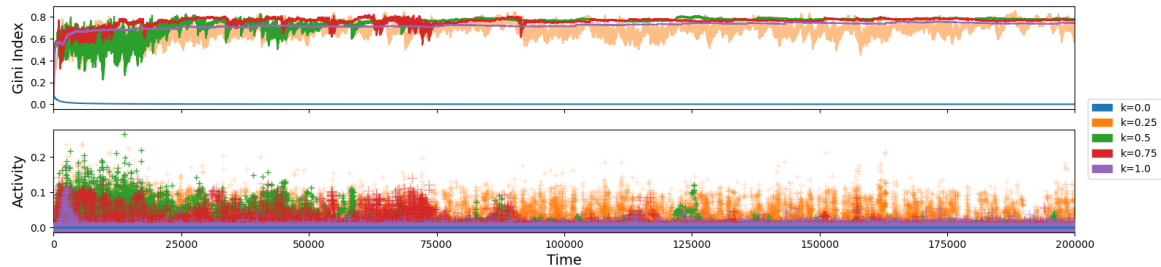

Figure 5.3: **Destructiveness Constant (k) Variation:** Temporal evolution of Gini index and commitment's activity. $\gamma = 0.7$, other parameters are as described in Table 3

On the other hand, we chose to vary the harvest parameter r, using values of 0, 50, 100, 150, and 200 over 200000 time steps. We obtained Figure 5.4 using the same procedure as before. We identified that for r values of 0, 100, 150, and 200, the systems asymptotically stabilize their Gini index and present lower values of the activity of the commitments in the early time steps. However, notice that $r = 0$ produces the most unequal populations since we are not providing resources to the system, so one or at least two agents accumulate the only resources available. On the other hand, the low values of Gini indexes were found with r values of 100, 150, and 200, indicating that the more resources are provided, the more equal the population becomes. Nonetheless, at $r = 50$, the Gini index and the activity of commitments present significant variability and high inequality. Overall, we identified that low
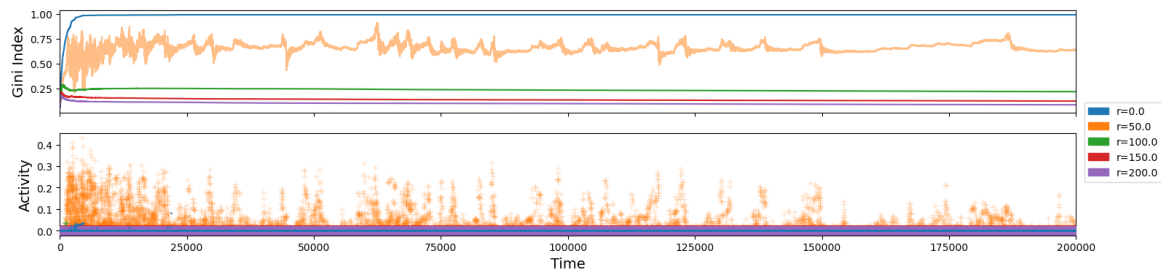
Figure 5.4: **Harvest Constant (r) Variation:** Temporal evolution of Gini index and commitment's activity. $\gamma = 0.7$, other parameters are as described in Table 3

activities of the commitment matrix stabilize the Gini index. We also determined that for values near $k = 0.25$ or $r = 50$, during the first 200000 time steps, the systems present more remarkable dispersion in the Gini index with high activity in the commitment matrix. Remember that conflicts influence commitments more, so under this range of parameters, such as the ones used in Chapter 1, we are under systems that also conflict with high inequality. On

the other hand, we identified that r plays an essential role in the distribution of resources, in which some values could
lower and stabilize the Gini indexes.

Finally, we constructed phase diagrams by initiating a transient of 10^4 steps to allow the system to reach a more
stable state. This was followed by averaging over the subsequent 10^4 steps. This process was repeated across 20
realizations, and the results were averaged to enhance statistical reliability. We observed that high activity and
dispersion of the commitment matrix stabilize the Gini index. Consequently, we calculate the mean of the Gini index
G as:

$$\bar{G} = \frac{1}{n} \sum_{i=1}^{n} G(t_i)$$

Meanwhile, the standard deviation of the activity $A(t)$ is given by:

$$\sigma_A = \sqrt{\frac{1}{n} \sum_{i=1}^{n} (A(t_i) - \bar{A})^2}$$

Both having $n = 10^4$ and t_i running from 10^4.

Figure 5.5 presents the phase diagrams of the Gini index and dispersion of the commitment matrix under the
variation of destructiveness (k) and harvest (r) parameters.

Figure 5.5: **Phase diagram: Destructiveness (k)- Harvest (r)** Comparative analysis of Gini index (a) and commit-
ment's activity variability (b). Other parameters are listed in Table 3.

In Figure 5.5(a), we observe a clear transition towards a more equitable distribution of resources as the harvest
parameter r varies. Interestingly, the destructiveness constant k does not significantly impact this distribution.
However, a slight increase in the orange zone at the inter-phase could be attributed to lower values of k ($k < 0.5$). To
confirm this, we would need to increase the resolution of the diagram. As expected, we observe a high Gini index

for $r = 0$, which leads to resource accumulation by a single agent, thereby stagnating the dynamics of conflicts. Conversely, for $k = 0$, we observe the lowest Gini index. This is because the system will always opt to fight, leading to a lack of development of commitments among agents and stagnating the emergence of influential agents.

These two extreme cases are corroborated with Figure 5.5(b), where we observe low variability in the activities of the commitments. Furthermore, Figure 5.5(b) provides a clear overview of the influence of k and r. In general, low values of k and values of $r < 90$ approximately result in more dispersion in the activity rate. The first, k, could be explained such that high values of destructiveness would make targets find it more profitable to pay than to fight. In the case of r, introducing resources above this limit allows every agent to recover their status.

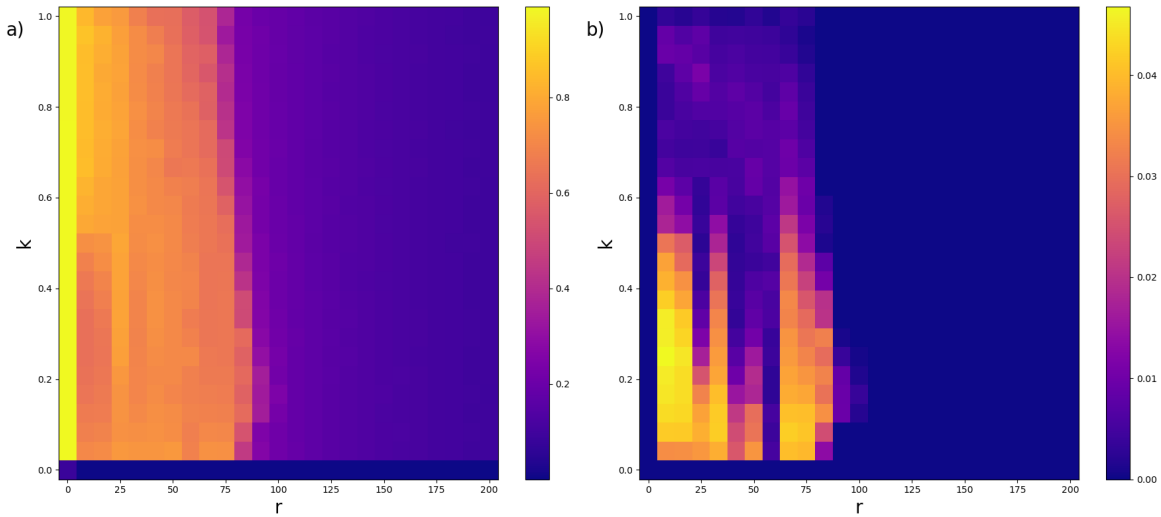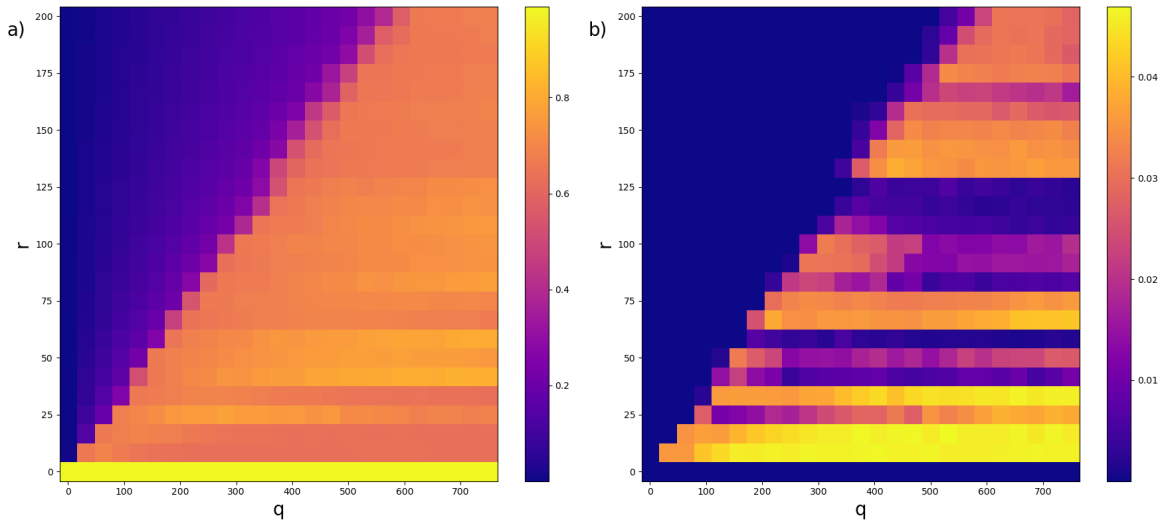Figure 5.6: **Phase diagram: Tribute (q)- Harvest (r)** Comparative analysis of Gini index (a) and commitment's activity variability (b). Other parameters are listed in Table 3.

On the other hand, Figure 5.6 shows the phase diagrams for the Gini index and activity for the variations of the tribute demanded (q) and harvest (r)). Figure 5.6(a) illustrates an interplay between q and r, delimiting high and low values transitions. The greater the tribute, the greater r should be to achieve a more evenly distributed system. As expected, extortion produces inequality (for any $q > 0$), and the higher the tribute payment, the more cost-effective it is to fight; hence, more resources should be administered to agents to defend their autonomy. Figure 5.6(b) shows specific bands of high dispersion of commitment activity, suggesting that certain levels of resources can mitigate the effects of high tributes, possibly reducing conflicts. In general terms, under this range of q, values of r under 30 produce more dispersion in the activity of commitments, and this activity corresponds to a relatively low Gini index shown in Figure 5.6(a).

In short, we reveal a transition to a more equitable population by adjusting mainly the harvest parameter r. However, the destructiveness constant k plays a pivotal role in the dispersion of commitment activity, and the effects of the tribute demanded value q are bounded by r. We also identify patches of the heatmap indicating fluctuations,

suggesting that other agents might influence this parameter.

We observe two distinct zones of high and low Gini indexes. In the high Gini region (orange), high dispersion of commitment activity results in relatively "lower" values, as conflicts lead to a redistribution of power. The low activity in this region indicates that resources are accumulated by a few agents, making it challenging for others to compete. However, it is essential to note that this relative difference in Gini values is only about 0.1, indicating that the system is still highly inequitable.

On the other hand, in the low Gini index region (purple), we observe a very low dispersion of activity, suggesting that fewer conflicts are occurring and more tribute payments are being made. However, the high periodic injection of resources prevents specific agents from standing out. This dynamic interplay between r, k, and q underscores the system's complexity and provides valuable insights into strategies for achieving a more equitable distribution of resources.

Chapter 6

Conclusions

Our research on Axelrod's Tribute Model has revealed a strong correlation between resource availability and tensions in a system of social, where scarcity of resources triggers conflicts and concentration. On the other hand, abundance of resources promotes equitable distribution of power through the emergence of new powerful agents. We have employed for the first time the Gini index as a global measure of inequality in conflict models. Notably, a high frequency of conflicts does not necessarily precipitate a sharp decline in the global economy. Instead, these conflicts can catalyze a restructuring of commitments among agents within and between coalitions, fostering the emergence of new powerful agents.

The analysis of conflicts in the 2-dimensional lattice model reveals that civil wars ($C_{ij} \geq 50\%$) are more prevalent, but non-civil ($C_{ij} < 50\%$) wars exhibit greater variability and extreme values. The distribution of the number of participants during conflicts follows a heavy-tailed distribution; i. e., a truncated power law with an exponent $\alpha = 1.57$ and an exponential truncation $\lambda = 0.01$. This behavior suggests that the participation of a few agents in conflicts is more probable, possibly due to dense commitments within coalitions.

We found that the inter-event time distributions of conflicts exhibits a bursty behavior, characterized by the formation of clusters of violent conflicts separated by periods of relative calm. We determined that log-normal distribution provides a better fit for all data regimes. In addition, no significant difference is observed between the log-normal and power law fits for the tail of the distribution. The observed patterns indicate the possible underlying processes driving the dynamics of conflicts.

We have shown the advantage of using complex network visualization tools to identify emergent aggregate agents in the commitment networks, offering a more intuitive approach than showing connectivity matrices. However, the matrix approach remains valuable, particularly for revealing the effects of the network topology, such as the tendency of commitments to grow locally in a 2-dimensional lattice.

The formation of a dominant aggregates of agents is observed, with extortion serving as a mechanism of resource accumulation. Civil wars play a crucial role in weakening the power of dominant aggregate agents by facilitating the restructuring of commitments and resources, thereby providing opportunities for others to emerge.

The Landscape Theory of Aggregation provides a plausible method to calculate the energy configuration and

explain wealth accumulation. It suggests that one way to reduce frustration and achieve system stability is by increasing the resources of coalition members. This comprehensive analysis offers valuable insights into societal tensions, conflicts, and the balance of power.

We have also investigated Axelrod's Tribute Model on a global network, where any agent can interact with any other. In contrast with the 2-dimensional square lattice configuration, the dynamics on a global network exhibits a higher frequency of conflicts and a decrease of overall resources. This could be attributed to the scarcity of global resources, which prevents high resource accumulation and leads to an unstable power structure. The Gini index for the global network is 0.72, while 0.86 for the 2-dimensional square lattice. The high Gini index values in both structures can be explained by the inherent nature of the model, particularly the "extortion" mechanism.

Civil wars are more frequent but relatively consistent across years, while non-civil conflicts, though less frequent, can be unpredictable and vary greatly in intensity. The distribution of participants in disruptions in the global network fits better with a log-normal distribution. The transition from a 2-dimensional lattice to a global network shifts from localized to global interactions, and this change in the interaction range has implications for the dynamics of the systems, including the rate and pattern of information propagation, as seen in the flow of resources. The importance of employing alternative visual methodologies, such as constructing an adaptive network of commitments, is emphasized to understand and to interpret complex interactions within the network.

Finally, the Probability Mass Function of the Manhattan distances of the 2-dimensional lattice exhibits an exponential decay behavior, allowing for flexible modeling of spatial interactions, capturing meaningful interactions, and maintaining computational efficiency. The harvest parameter r plays a crucial role in the distribution of resources, with some values potentially lowering and stabilizing the Gini indexes. However, the destructiveness constant k significantly influences the dispersion of commitment activity, and the effects of the tribute demanded value q are bounded by r.

Our findings can contribute to the development of strategies for conflict management and resource allocation in different social network structures.

Appendix A

Appendix: Tribute Model

All code used to replicate the analyses detailed in this document is included here. Furthermore, a comprehensive collection of scripts and data files can be found at the following GitHub repository: https://github.com/brandonminta/conflictmodel

The repository includes scripts written in Python, along with additional resources essential for reproducing the reported results. For questions or support related to the code or its execution, please consult the GitHub repository or reach out to the author directly.

Listing A.1: Tribute model

```python
#!/usr/bin/env python
# @author: Brandon Minta
# ————————————————————————————————
#
#   A simulation of a socio-dynamical model of conflicts based on
#   "pay or else" for simple interaction rules among in different
#   toplogies
#
# ————————————————————————————————
import argparse
import os

import numpy as np
import math
import h5py
from tqdm import tqdm
import multiprocessing as mp
import networkx as nx
```

```python
import random
# ———————————————————————————————————————————————————————————————
def parse_arguments():
    parser = argparse.ArgumentParser(description='Run the simulation script.')
    parser.add_argument('-N', type=int, default=100, help='Number of actors')
    parser.add_argument('--years', type=int, default=1000, help='Number of \
    iterations')
    parser.add_argument("--network_type", choices=["watts_strogatz", "grid_2d",
    "complete", "wheel"], default="grid_2d", help="Type of network")
    parser.add_argument('--ncpu', type=int, default=1, help='Number of \
    processes')
    parser.add_argument("--output_dir", required=True, help="Output directory")
    return parser.parse_args()
#Constants
args =  parse_arguments()
c = 1                           # commitment fluctuation
k = 0.25                        # Destructiveness
demands = 3                     # Demands per Year Cycle (1/3 of N)
period_steps = 1                # Period for data collection
r = 20                          # harvest
q = 250                         # Tribute


def saving_data(rank, output_dir, loyalty_list, data_matrix):
    subdirectory_name = f"run_{rank}"  # Create the subdirectory name
    subdirectory_path = os.path.join(output_dir, subdirectory_name)
    # Create the subdirectory if it doesn't exist (with exist_ok=True
    # it won't raise an error if it already exists)
    os.makedirs(subdirectory_path, exist_ok=True)
    # Save data to HDF5 files
    with h5py.File(os.path.join(subdirectory_path, f"\
    loyalty_output_{rank}.h5"), 'w') as hf:
        for i, array in enumerate(loyalty_list):
            hf.create_dataset(f'loyalty_matrix_{i}', data = array)

    with h5py.File(os.path.join(subdirectory_path, f"\
    simulation_output_{rank}.h5"), 'w') as hf:
        hf.create_dataset('simulation_data', data = data_matrix)
```

```python
def create_graph(num_nodes, graph_type='grid', **kwargs):
    """
    Create and return a NetworkX graph based on the specified number
    of nodes and graph type.

    Parameters:
    num_nodes (int): Number of nodes in the graph.
    graph_type (str): Type of graph ('grid', 'scale_free',
    or 'watts_strogatz').
    **kwargs: Additional arguments specific to the chosen graph type.

    Returns:
    nx.Graph: NetworkX graph based on the specified parameters.
    """
    if graph_type == 'grid_2d':
        factors = []
        for i in range(1, int(math.sqrt(num_nodes)) + 1):
            if num_nodes % i == 0:
                factors.append((i, num_nodes // i))
        m, n = min(factors, key=lambda x: abs(x[0] - x[1]))
        G = nx.grid_2d_graph(m, n, periodic=True)
        mapping = {(i, j): i * n + j for i in range(m) for j in range(n)}
        G = nx.relabel_nodes(G, mapping)
    elif graph_type == 'watts_strogatz':
        k = kwargs.get('k', 4)  # Default value for k is set to 4
        p = kwargs.get('p', 0.1)  # Default value for p is set to 0.1
        G = nx.watts_strogatz_graph(num_nodes, k, p)
    elif graph_type == 'complete':
        G = nx.complete_graph(num_nodes)
    elif graph_type == 'wheel':
        G = nx.wheel_graph(num_nodes)
    return G

def loss(coAWealth, coBWealth, contribution):
    """
    The function calculates loss of resources from an actor of coalition B,
    caused by conflict with coalition A
```

```
    """
    return k*coAWealth*(contribution)/coBWealth

def vulnerability(r_i, r_j):
    """
    The function computes the vulnerability of agent j with respect to agent i
    """
    return (r_i - r_j) / r_i if r_i > 0 and r_j > 0 else 0

def group_resources(agent, coalition_arr, capital_arr, loyalty_mtx):
    """
    The function calculates the total resources of a coalition

    Parameters
    _____

    agent: int
        The group leader
    coalition_arr: array
        Coalition
    capital_arr: array
        Capital of each member
    loyalty_mtx: array
        Commitment matrix


    return
    _____

    money: float
        The total resources of the coalition

    """
    money = 0
    for i in coalition_arr:
        money += 0.1*loyalty_mtx[i][agent] * capital_arr[i]
    return money

def candidate_connection(G, loyalty_mtx, attacker, target):
    """
    This function checks is there is a path between Attacker and target
```

```python
    """
    # Create a subgraph to remove nodes
    H = G.copy()
    nodes_to_isolate = []   #node more committed with target
    for node in range(len(loyalty_mtx)):
        conditionA = loyalty_mtx[node, attacker]
        conditionB = loyalty_mtx[node, target]
        if (conditionA <= conditionB ) and node not in [attacker, target]:
            nodes_to_isolate.append(node)
    H.remove_nodes_from(nodes_to_isolate)
    #Check if there is a path between nodes
    if nx.has_path(H, attacker, target):
        path_length = nx.shortest_path_length(H, source=attacker,
        target=target)
        return path_length
    else:
        return None


def group(G, a, b, loyalty_mtx):
    """
    This function find the spatial connected coalition of 'a'
    """
    # Create an initial grouping where each node is its own group
    group_a = {node for node in G.nodes() if
            (loyalty_mtx[node, a] > loyalty_mtx[node, b] and
                node != b) or (node == a)}
    subgraph = G.subgraph(group_a)
    coalition = list(nx.descendants(subgraph, a))+ [a]
    return np.array(coalition, dtype=int)


def group_global(a, b, loyalty_mtx):
    loyalty_to_a = loyalty_mtx[:, a]
    loyalty_to_b = loyalty_mtx[:, b]
    group_a = np.where(loyalty_to_a > loyalty_to_b)[0]
    group_b = np.where(loyalty_to_b > loyalty_to_a)[0]
    # Include "a" in group_a and "b" in group_b
    group_a = np.union1d(group_a, [a])
    group_b = np.union1d(group_b, [b])
```

```python
    return group_a, group_b

def candidate_exposure(G, attacker, target, capital, loyalty_mtx, path_length):
    """
    This function calculates the susceptibility
    """
    attacker_alley = group(G, attacker, target, loyalty_mtx)
    target_alley = group(G, target, attacker, loyalty_mtx)
    w_att = group_resources(attacker, attacker_alley, capital, loyalty_mtx)
    w_def = group_resources(target, target_alley, capital, loyalty_mtx)
    susceptibility = vulnerability(w_att, w_def) * min(q, capital[target])
    return susceptibility, attacker_alley, target_alley, w_att, w_def

def candidate_selection(G, loyalty_mtx, attacker, capital, network_type):
    """
    This function selects the best target possible if any
    """
    if network_type == 'complete':
        def get_optimal_params(target):
            attacker_alley, target_alley = group_global(attacker,
                                                target, loyalty_mtx)
            w_att = group_resources(attacker, attacker_alley, capital,
                    loyalty_mtx)
            w_def = group_resources(target, target_alley, capital,
                    loyalty_mtx)
            susceptibility = vulnerability(w_att, w_def) * min(q,
                            capital[target])
            return {
                "susceptibility": susceptibility,
                "attacker_alley": attacker_alley,
                "target_alley": target_alley,
                "w_att": w_att,
                "w_def": w_def,
                "target": target,
                "attacker": attacker,
                "path_len":None
                }
```

```python
        optimal = {
            "susceptibility": 0,
            "attacker_alley": None,
            "target_alley": None,
            "w_att": None,
            "w_def": None,
            "target": None,
            "attacker": None,
            "path_len":None
        }

        for i in range(len(loyalty_mtx)):
            if i != attacker:
                params = get_optimal_params(i)
                if params["susceptibility"] > optimal["susceptibility"]:
                    optimal.update(params)

        return optimal
    else:
        neighbors_attacker = list(G.neighbors(attacker))
        params
        def get_optimal_params(target):
            """
            Helper function to calculate susceptibility and other
            parameters for a target node.
            """
            path_length = candidate_connection(G, loyalty_mtx, attacker,
            target)
            # Exclude not profitable targets and not spatially connected.
            if capital[target] < 0.1 or path_length is None:
                return {
                "susceptibility": 0,
                "attacker_alley": None,
                "target_alley": None,
                "w_att": None,
                "w_def": None,
                "target": None,
```

```
            "attacker":None,
            "path_len":None
        }
        # Calculate parameters using candidate_exposure function
        susceptibility, attacker_alley, target_alley, w_att, w_def =
        candidate_exposure(G, attacker, target, capital,
        loyalty_mtx, path_length)
        return {
            "susceptibility": susceptibility,
            "attacker_alley": attacker_alley,
            "target_alley": target_alley,
            "w_att": w_att,
            "w_def": w_def,
            "target": target,
            "attacker":attacker,
            "path_len":path_length
        }

# Initialize optimal parameters with the first neighbor of the attacker
optimal = get_optimal_params(neighbors_attacker[0])
# Iterate through other neighbors of the attacker and update optimal
# parameters if a better target is found
for target in neighbors_attacker[1:]:
    params = get_optimal_params(target)
    # Check if the target is valid and has higher susceptibility
    if params and params["susceptibility"] > optimal["susceptibility"]:
        optimal.update(params)

# Iterate through all nodes that are not neighbors of the attacker
# and update optimal parameters if a better target is found
for target in [node for node in range(len(loyalty_mtx)) if
    node not in neighbors_attacker and node != attacker]:
    # Check if target's neighbors are not commited with attacker
    #(no possible path)
    if all(loyalty_mtx[node][attacker] <= loyalty_mtx[node][target] for
        node in list(G.neighbors(target))):
        continue
    params = get_optimal_params(target)
```

```python
            # Update optimal parameters if a better target is found
            if params and params["susceptibility"] > optimal["susceptibility"]:
                optimal.update(params)


        # Return the optimal parameters
        return optimal


def response(optimal, capital, loyalty_mtx):
    attacker = optimal["attacker"]
    target = optimal["target"]
    w_def = optimal["w_def"]
    w_att = optimal["w_att"]
    target_alley = optimal["target_alley"]
    attacker_alley = optimal["attacker_alley"]
    damage_by_attacker = min(k*w_att, w_def)   #can't cause more damage
    damage_by_defender = min(k*w_def, w_att)
    loyalty = np.copy(loyalty_mtx[attacker][target])
    activity = 0
    #Consider only target's damage
    if min(q, capital[target]) > (damage_by_attacker*capital[target]/w_def):
        for i in target_alley:
            offering = 0.1*loyalty_mtx[i][target] * capital[i]
            contribution_loss = damage_by_attacker*offering/w_def
            capital[i] -= contribution_loss
            for m in target_alley:
                if 10 - c >= loyalty_mtx[i][m] >= 0:
                    loyalty_mtx[i][m] = loyalty_mtx[i][m] + c
                    activity += 1
            for n in attacker_alley:
                if 10 >= loyalty_mtx[i][n] >= c:
                    loyalty_mtx[i][n] = loyalty_mtx[i][n] - c
                    loyalty_mtx[n][i] = loyalty_mtx[n][i] - c
                    activity += 2

        for j in attacker_alley:
            offering = 0.1*loyalty_mtx[j][attacker] * capital[j]
            contribution_loss = damage_by_defender*offering/w_att
            capital[j] -= contribution_loss
```

```python
            for l in attacker_alley:
                if 10 - c >= loyalty_mtx[j][l] >= 0:
                    loyalty_mtx[j][l] = loyalty_mtx[j][l] + c
                    activity += 1
        # Conflict: True ; Loyalty between attacker and target, activity
        return 1, loyalty, activity/2
    else:
        money = min(q, capital[target])
        capital[target], capital[attacker] = capital[target] - money,
        capital[attacker] + money
        if 10 - c >= loyalty_mtx[target][attacker] >= 0 :
            loyalty_mtx[target][attacker] += c
            loyalty_mtx[attacker][target] += c
            activity += 2
        # Conflict: False ; Loyalty between attacker and target, activity
        return 0, loyalty, activity/2


# Simulation ─────────────────────────────────────────────────
class Simulation:
    def __init__(self, N, years, G, rank, network_type):
        self.rank = rank
        self.N = N                                      # Number of actors
        self.years = years                              # Years
        self.G = G                                      # Network
        self.capital = np.zeros(self.N)                 # Wealth
        self.loyalty_mtx = np.identity(self.N, dtype= int)*10
        self.network_type = network_type
    def simulate_activation(self):
        attacker = random.randrange(0, self.N)
        optimal = candidate_selection(self.G, self.loyalty_mtx, attacker,
        self.capital, self.network_type)
        if optimal["susceptibility"] > 0:    #Target
            decision, loyalty, activity = response(optimal, self.capital,
            self.loyalty_mtx)
            return decision, loyalty, optimal, activity
        else:
            return None, None, optimal, 0
```

```python
def run_simulation(self, pbar = None):
    #Get the total number of iterations
    total_iterations = self.years * (self.N // demands)
    #Initialize the resources for each actor
    for i in range(self.N):
        self.capital[i] = random.randrange(300,500,1)
    loyalty_list = [] # Lists for periodic loyalty
    data_matrix = np.zeros((total_iterations+1, self.N + 10),
                    dtype=np.float32)
    data_matrix[0,10:] = self.capital
    #Create the charging bar if pbar is provided
    if pbar:
        pbar.reset(total=total_iterations)
    # Loop for each simulation run
    iterator, period = 1, period_steps
    for year in range(self.years):
        if self.rank == 1:
            loyalty_list.append(np.copy(self.loyalty_mtx))
        for k in range(self.N // demands):
            decision, loyalty, optimal, activity = (
                self.simulate_activation())
            if decision is not None:
                # Perform element-wise comparison and count
                # the number of differing elements)
                info = np.array([decision, optimal["attacker"],
                optimal["target"], loyalty,
                        len(optimal["target_alley"]),
                        len(optimal["attacker_alley"]), optimal["w_def"],
                        optimal["w_att"], optimal["path_len"], activity])
            else:
                info = np.full(10, None)
            data_matrix[iterator,:10], data_matrix[iterator,10:] = info,
                self.capital
            iterator += 1
            if pbar:
                pbar.update(1)
        self.capital += r
```

```python
        loyalty_list.append(np.copy(self.loyalty_mtx))
        return loyalty_list, data_matrix


def run(rank, output_dir, N, years, G, network_type):
    simulation = Simulation(N, years, G, rank, network_type)
    with tqdm(total=total_iterations, desc="Simulation Progress",

    unit="iteration") as pbar:
        loyalty_list, data_matrix = simulation.run_simulation(pbar=pbar)
        saving_data(rank, output_dir, loyalty_list, data_matrix)


if __name__ == "__main__":
    args = parse_arguments()
    N = args.N
    years = args.years
    network_type = args.network_type
    output_dir = args.output_dir
    ncpu = args.ncpu

    network = create_graph(N, graph_type = network_type)
    total_iterations = years * (N // demands)
    # Create output directory if it doesn't exist
    os.makedirs(output_dir, exist_ok=True)

    # Get number of laptop CPUs
    n_cpu = mp.cpu_count()
    # Call Pool
    pool = mp.Pool(processes=ncpu)
    # Create a list of tuples containing all combinations of paramters
    parameters = [(rank, output_dir, N, years, network, network_type) for
        rank in range(1,ncpu+1)]
    # Call run for all parameter tuples using pool.map
    pool.starmap(run, parameters)
    # Close the pool
    pool.close()
```

Bibliography

[1] da Cunha, C. R. *Introduction to Econophysics: Contemporary Approaches with Python Simulations*; CRC Press, 2021.

[2] Jensen, H. J. *Complexity science: the study of emergence*; Cambridge University Press, 2022.

[3] Sayama, H. *Introduction to the modeling and analysis of complex systems*; Open SUNY Textbooks, 2015.

[4] Sen, P.; Chakrabarti, B. K. *Sociophysics: an introduction*; OUP Oxford, 2014.

[5] Gilbert, N.; Conte, R. *Artificial societies*; Taylor & Francis, 1995.

[6] Von Neumann, J.; Morgenstern, O. Theory of games and economic behavior, 2nd rev. **1947**,

[7] Axelrod, R. Building new political actors. *Robert Axelrod, The Complexity of Cooperation* **1997**, 121–44.

[8] Newman, M. *Networks*; Oxford university press, 2018.

[9] Kreis, R. The "tweet politics" of President Trump. *Journal of language and politics* **2017**, *16*, 607–618.

[10] Zachary, W. W. An information flow model for conflict and fission in small groups. *Journal of anthropological research* **1977**, *33*, 452–473.

[11] Moreno, J. L. Who shall survive? A new approach to the problem of human interrelations. **1934**,

[12] Blondel, V. D.; Guillaume, J.-L.; Lambiotte, R.; Lefebvre, E. Fast unfolding of communities in large networks. *Journal of statistical mechanics: theory and experiment* **2008**, *2008*, P10008.

[13] Axelrod, R. *The Complexity of Cooperation: Agent-Based Models of Competition and Collaboration: Agent-Based Models of Competition and Collaboration*; Princeton university press, 1997.

[14] Schelling, T. C. Dynamic models of segregation. *Journal of mathematical sociology* **1971**, *1*, 143–186.

[15] Axelrod, R. Effective choice in the prisoner's dilemma. *Journal of conflict resolution* **1980**, *24*, 3–25.

[16] Alstott, J.; Bullmore, E.; Plenz, D. powerlaw: a Python package for analysis of heavy-tailed distributions. *PloS one* **2014**, *9*, e85777.

[17] Herrera, J. L.; Cosenza, M. G.; Tucci, K. Stratified economic exchange on networks. *Physica A: Statistical Mechanics and its Applications* **2011**, *390*, 1453–1457.

[18] Karsai, M.; Kaski, K.; Barabási, A.-L.; Kertész, J. Universal features of correlated bursty behaviour. *Scientific reports* **2012**, *2*, 397.

[19] Vázquez, A.; Oliveira, J. G.; Dezsö, Z.; Goh, K.-I.; Kondor, I.; Barabási, A.-L. Modeling bursts and heavy tails in human dynamics. *Physical Review E* **2006**, *73*, 036127.

[20] Picoli, S.; Castillo-Mussot, M. d.; Ribeiro, H. V.; Lenzi, E.; Mendes, R. Universal bursty behaviour in human violent conflicts. *Scientific reports* **2014**, *4*, 4773.

[21] Picoli, S.; Antonio, F. J.; Itami, A. S.; Mendes, R. S. Power-law relaxation in human violent conflicts. *The European Physical Journal B* **2017**, *90*, 1–5.

[22] Barabasi, A.-L. The origin of bursts and heavy tails in human dynamics. *Nature* **2005**, *435*, 207–211.

[23] Bak, P.; Christensen, K.; Danon, L.; Scanlon, T. Unified scaling law for earthquakes. *Physical Review Letters* **2002**, *88*, 178501.

[24] Baró, J.; Corral, Á.; Illa, X.; Planes, A.; Salje, E. K.; Schranz, W.; Soto-Parra, D. E.; Vives, E. Statistical similarity between the compression of a porous material and earthquakes. *Physical review letters* **2013**, *110*, 088702.

[25] Stouffer, D. B.; Malmgren, R. D.; Amaral, L. A. Comment on Barabasi, Nature 435, 207 (2005). *arXiv preprint physics/0510216* **2005**,

[26] Karsai, M.; Jo, H.-H.; Kaski, K. *Bursty Human Dynamics*; Springer International Publishing: Cham, 2018; pp 47–71.

[27] Masoliver, J.; Montero, M.; Weiss, G. H. Continuous-time random-walk model for financial distributions. *Physical Review E* **2003**, *67*, 021112.

[28] Malmgren, R. D.; Stouffer, D. B.; Campanharo, A. S.; Amaral, L. A. N. On universality in human correspondence activity. *science* **2009**, *325*, 1696–1700.

[29] Fang, Z.; Wang, J.; Liu, B.; Gong, W. Double Pareto lognormal distributions in complex networks. *Handbook of Optimization in Complex Networks: Theory and Applications* **2012**, 55–80.

[30] Reed, W. J.; Jorgensen, M. The double Pareto-lognormal distribution—a new parametric model for size distributions. *Communications in Statistics-Theory and Methods* **2004**, *33*, 1733–1753.

[31] Downey, A. B. Lognormal and Pareto distributions in the Internet. *Computer Communications* **2005**, *28*, 790–801.

[32] Mitzenmacher, M. A brief history of generative models for power law and lognormal distributions. *Internet mathematics* **2004**, *1*, 226–251.